Pentalinonsterol, Scytonemide A, and Structural Analogues as Mechanistic Probes for the Exploration of Antileishmanial/Anti-Cancer Activities

Undergraduate Research Thesis

Presented in Partial Fulfillment of the Requirements for Graduation "with Honors Research Distinction in Biochemistry" in the undergraduate colleges of The Ohio State University

By

Robert M. Demoret

The Ohio State University

2015

Project Advisor: Professor James R. Fuchs, Department of Medicinal Chemistry and Pharmacognosy

Acknowledgments

The authors would like to gratefully acknowledge the Arts and Sciences Undergraduate Research Scholarship, NIH Grants AI 076309, AT 004160, 542 AI 090803 (to A.R.S.), RC4 AI 092624 (to A.R.S. and A.D.K.), DOD Grant W81XWH-14-2-0168 (to A.R.S.), as well as the P01 CA125066 for the funding of these projects.

Vita

2015.....B.S.

Publications

N.A.

Poster Awards

1st Place Denman Undergraduate Research Forum (Biological Sciences Category)……... 2014

4th Place Denman Undergraduate Research Forum (Biological Sciences Category)…….. 2015

Fields of Study

Major Field: Biochemistry

Table of Contents

List of Tables

List of Figures

List of Schemes

Part I: Synthesis, optimization and evaluation of pentalinonsterol and its analogues for structure-activity relationship studies

Chapter 1: Leishmanisis: The world's second deadliest parasite

Leishmaniasis is the world's second deadliest parasite with an estimated 1.3 million new cases every year and death totals that range from 20,000-30,000 per year[1]. It is a vector-borne disease that is typically spread by the bite of the female phlebotomine sandfly. The females require blood for their eggs and they acquire and transmit the disease when they feed[2]. Human infection is caused by approximately 21 to 30 different species of sandflies which are endemic to intertropical and temperate regions of the world[2].

The leishmania parasite can be found in two different stages: The promastigote stage (infective stage) and the amastigote stage (proliferative tissue stage). These stages of the parasitic life cycle are illustrated in **Figure 1**. When an infected sandfly takes a bloodmeal it injects

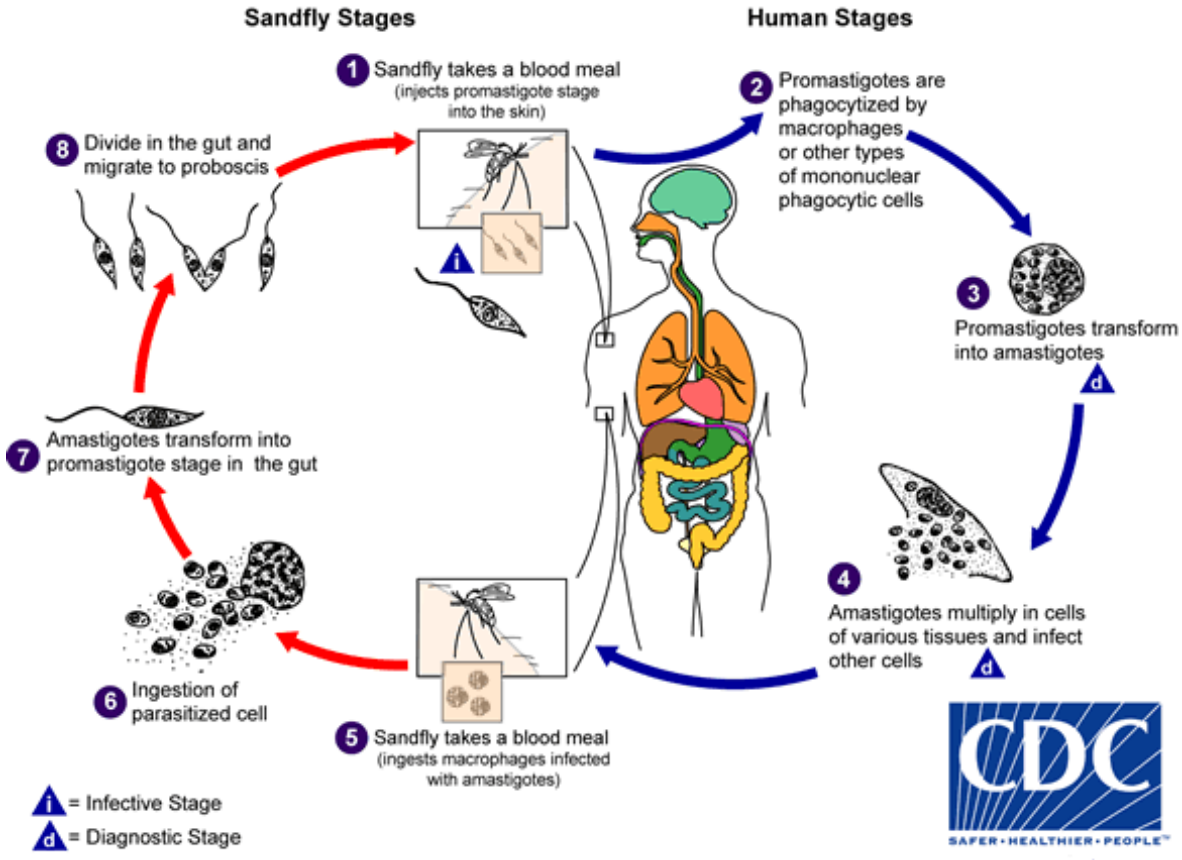

Figure 1

promastigotes into the blood which are then phagocytized by macrophages or other mononuclear phagocytotic cells. Once the parasite has been phagocytized it transforms into the amastigote which then proliferates within the phagocytotic cells. Since the amastigotes replicate continually the phagocytotic cells usually undergo cellular lysis which releases the amastigotes into the blood stream which are then phagocytized or infect other cells. When a sandfly takes a bloodmeal from an infected human it ingests infected macrophages which then release the amastigotes into the sandfly. Within the sandfly the amastigotes transform back into the promastigote where they can then be transmitted back to a human after another bloodmeal[3].

It is possible for an infected host to never develop the disease; however, leishmaniasis can present itself with symptoms in three different forms: cutaneous, mucocutaneous, and visceral leishmaniasis.

- Cutaneous leishmaniasis (CL) is the most common form of the disease and causes skin lesions, typically in the form of an ulcer. These lesions can develop as quickly as several weeks or take years to appear. The ulcers are non-lethal however they can becomes infected which may lead to discomfort, life-long scars other medical problems[1,4].
- Mucocutaneous leishmaniasis (ML) is a result of leaving cutaneous leishmaniasis untreated which allows the disease to spread to the naso-oropharyngeal mucosa (mucous membranes of the nose, mouth, and throat). The symptoms involve bleeding of the infected area which can then become ulcerous leading to ulcerative destruction[1,4].
- Visceral leishmaniasis (VL, a.k.a. kala-azar) is the fatal form of leishmaniasis when it is left untreated. Visceral leishmaniasis is found in internal organs and has a list of symptoms that include weights loss, fever, hepatomegaly and /or splenomegaly, pancytopenia. Both the direct effects and secondary effects, such as hemorrhage or secondary infection, are fatal[1,4].

After looking at maps depicting the worldwide distribution of leishmaniasis **(Figure 2[5]),** it is fairly obvious why leishmaniasis is one of the seventeen prioritized Neglected Tropical

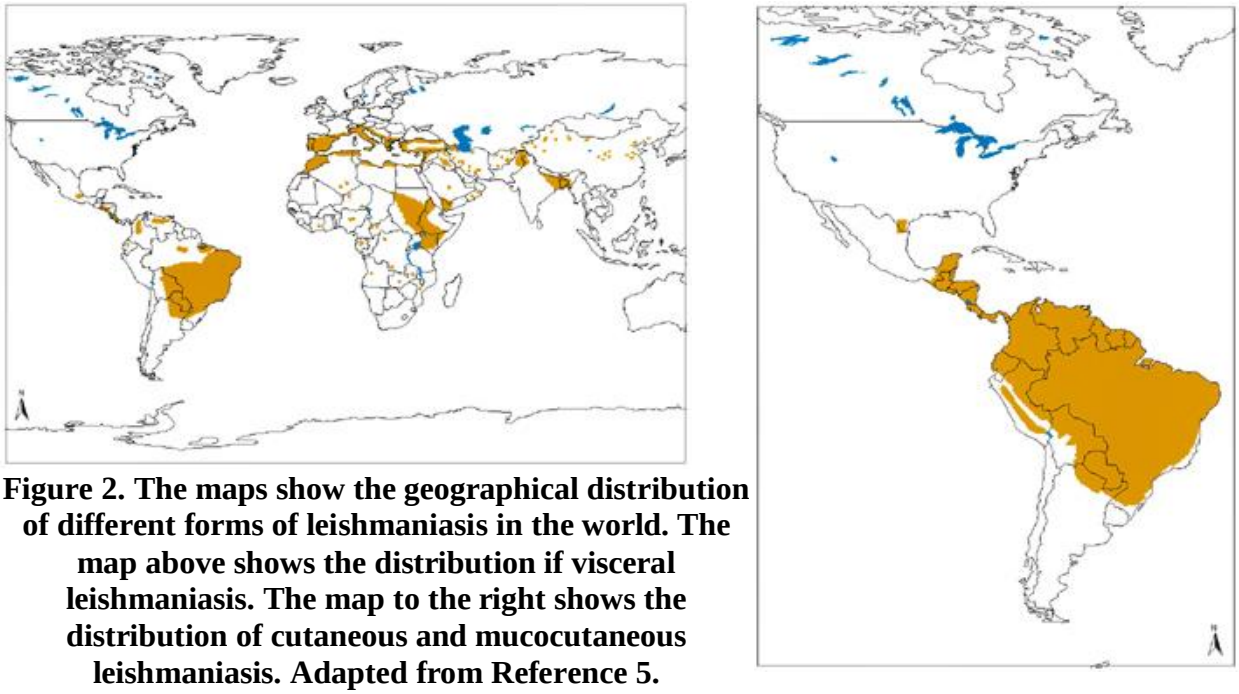

Figure 2. The maps show the geographical distribution of different forms of leishmaniasis in the world. The map above shows the distribution if visceral leishmaniasis. The map to the right shows the distribution of cutaneous and mucocutaneous leishmaniasis. Adapted from Reference 5.

diseases (NTD) . The CDC defines a NTD as any group of parasitic and bacterial diseases that cause substantial illness for more than one billion people globally[6] and leishmaniasis falls into this category. NTD's affect the world's poorest countries and people; making diagnostics, treatments, administration, and logistics more difficult. Long-term monitoring of the disease is also a major problem. It is important to monitor for relapse or recrudescence in patients who have overcome the disease because drug resistant strains are beginning to appear in areas such as Bihari-India and south-east Nepal. Patients with more severe cases of leishmaniasis require more intensive therapies which are very difficult due to administration (intravenous injection), and expensive in third world countries. Leishmaniasis is also one of the NTD's that has limitations on the large scale use of the existing therapies and treatment methods[7].

Current Therapies

Antimonials

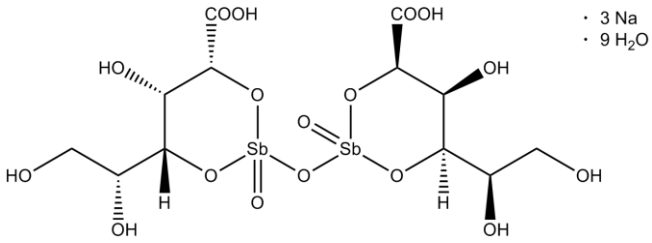

Sodium Stibogluconate (Pentostam)

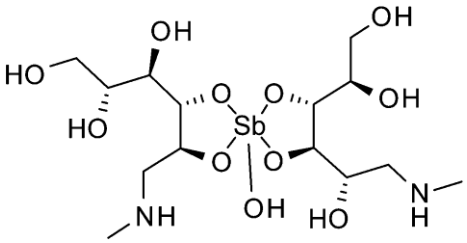

Glucantime

Pentavalent antimonial drugs have been the first-line of defense against leishmaniasis worldwide for over 75 years. Pentostam® and Glucantime® (seen above) are the two current drugs that are approved for clinical use. These drugs are administered intravenously at 20 mg/kg/day up to 1275 mg over 20 or 30 days. The trivalent antimonial is the pharmacophore that kills the parasites through alteration of their biopathways. Side effects of the antimonials include nausea, diarrhea, vomiting, malaise, myalgia, and anorexia. The cure rate for these drugs is roughly 85-95% except in countries that have resistant strains to these drugs[8].

Amphotericin B

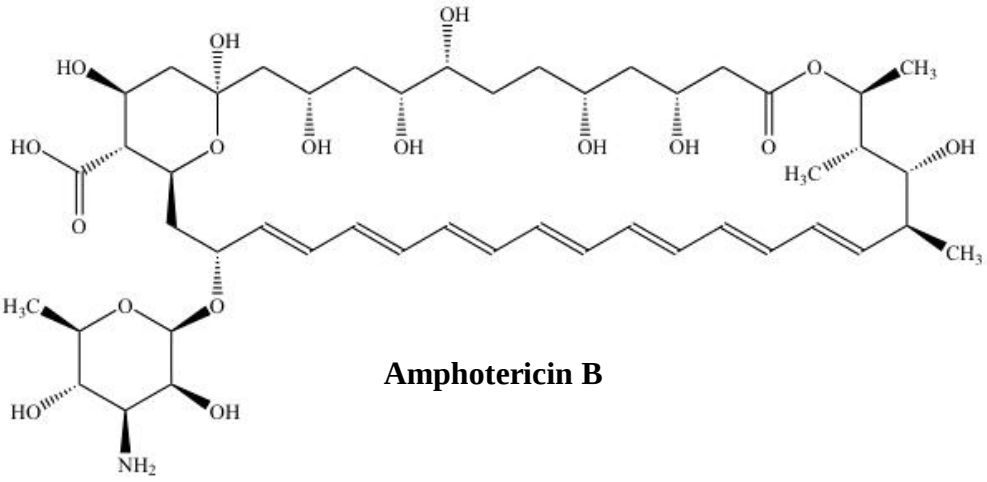

Amphotericin B

Amphotericin B is a macrolide polyene that is used commonly in locations where antimonial resistance is prevalent. The drug is encapsulated in a liposome and then administered intravenously at 7-20mg/kg/day for up to 20 days. Amphotericin B binds to membrane ergosterol which results in pore formation and ultimately parasite cell lysis. The major side effect of this drug is renal toxicity, which can be reduced through the use of a liposomal derivative of this drug. However, both of these drugs are expensive which limits their use in developing countries[8].

Miltefosine

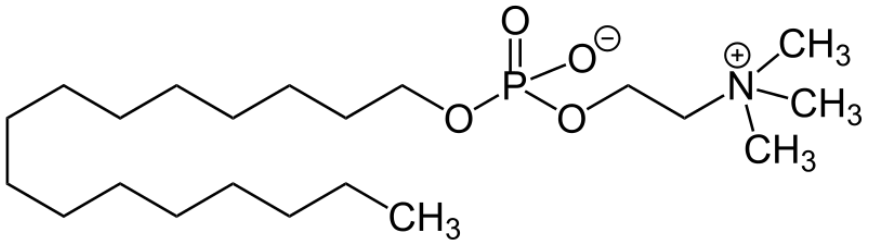

Miltefosine

Miltefosine is one of the newest drugs on the market and is derived from cancer therapeutics. This drug is thought to alter multiple pathways within the parasite such as signal transduction and glycosylphosphatidylinositol anchor (GPI) synthesis. This was the first approved anti-leishmanial drug that could be administered orally, which has led to extremely high cure rates in both CL and VL at 100-150mg/day for 28 day doses. Side effects include nausea and vomiting, but overall are quite mild[8].

Natural Products as Drugs

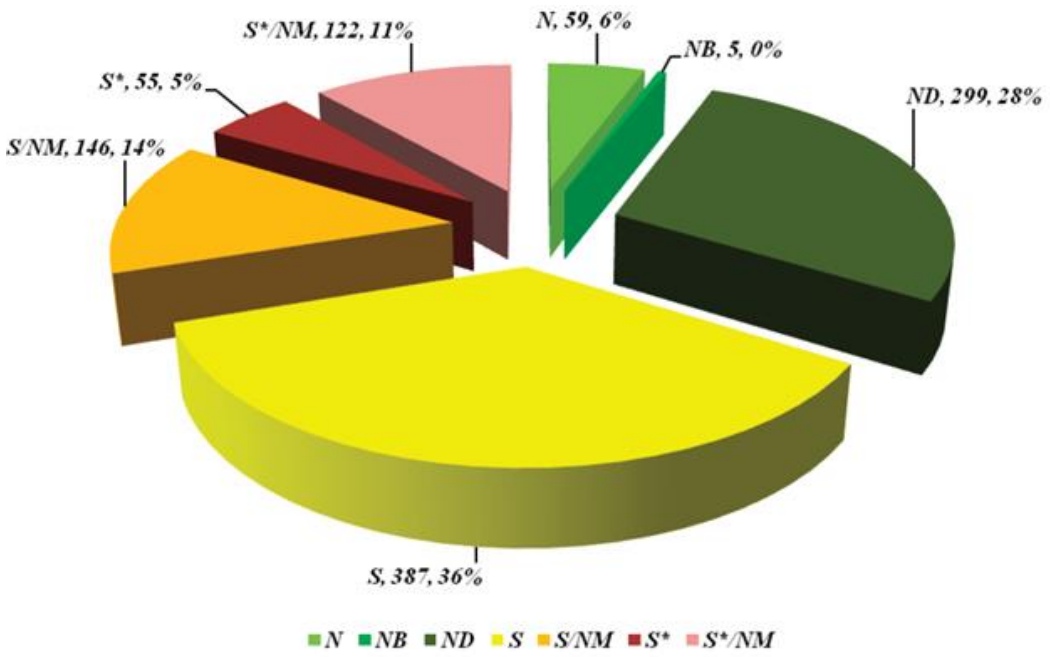

Figure 3 Newman, D. J.; Cragg, G. M. *J. Nat. Prod.* 2012, *75*, 311–335.

It becomes apparent after looking at the current antileishmanial therapies that new drugs are needed that are less toxic and expensive. While the use of high-throughput screening with large combinatorial libraries has gained popularity in recent years, natural products, or their derivatives, are still the major source of leads as drug molecules[9]. It can be seen in **Figure 3** that only 36% of new approved small molecule drugs since 1981 are purely synthetic. 64% of new small molecule drugs since 1981 are natural products or derived from these species. From 1981 to 2010 only 14 antiparasitic compounds have been approved as drugs and 9 of them were natural products or related derivatives[9]. Since a majority of these compounds are natural products it emphasizes the importance to continue utilizing natural sources as a means of discovery for novel antiparasitic secondary metabolites.

Chapter 2: The Discovery, biological evaluation, and structure activity relationship study of Pentalinonsterol

The Discovery and Chemical Analysis of Pentalinonsterol

Ancient Mayans utilized the roots of *Pentalinon Adrieuxii*, which is native to the Yucatan Peninsula in Mexico, as a means of treating leishmaniasis. The internal parts of the roots were applied to the lesions on the body and were reapplied daily until visible healing had occurred. Previous biological evaluations of this plant led to the discovery of other natural products with antileishmanial activity, which was of interest in the Kinghorn lab, one of our collaborators on this project at The Ohio State University[10]. The Kinghorn group utilized bioassay guided fractionation against the protozoa of *L. mexicana* in order to isolate the most active components of the *Pentalinon Adrieuxii* roots. During the course of isolation, the root material was extracted and fractionated using solvents of varying polarity. The hexanes extract was found to be most active of the partitions. It was also noted that topical treatment of infected mice ear cells with the hexanes extract of the *P. Adrieuxii* roots showed inhibition of leishmanial growth which can be seen below in **figure 6**. The control consisted of *L. Mexicana* infested macrophages of the mouse ear cells and it can be seen in the PARE treated

Figure 5 Air dried *Pentalinon Adrieuxii* roots

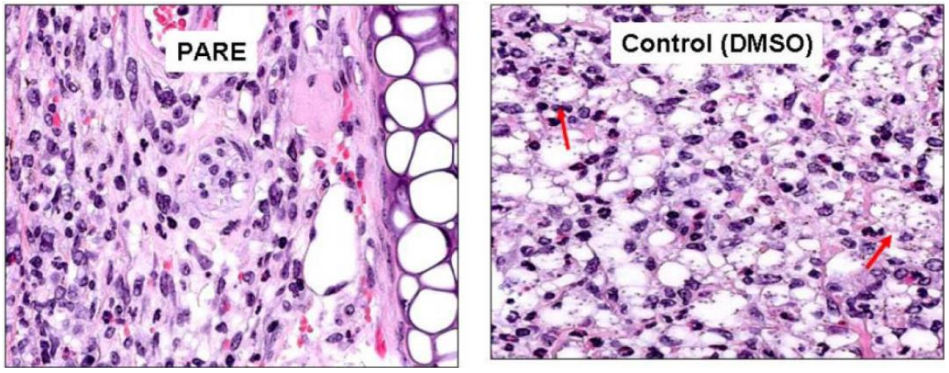

Figure 4 The effect of topical application of the hexane extract of the *P. andrieuxii* roots against *L. Mexicana*.

cells that the viral load has decreased. The PARE is the hexane extract which contains pentalinonsterol (PEN). Isolation and purification of the hexanes extract resulted in the identification of 20 compounds which were subsequently submitted for testing against *L. Mexicana*. **Figure 5** portrays the structures of the most active compounds from the screen. **Table 1** contains the names and activities of the respective compounds against both the amastigote and promastigote forms of the parasite with pentostam as the positive control.

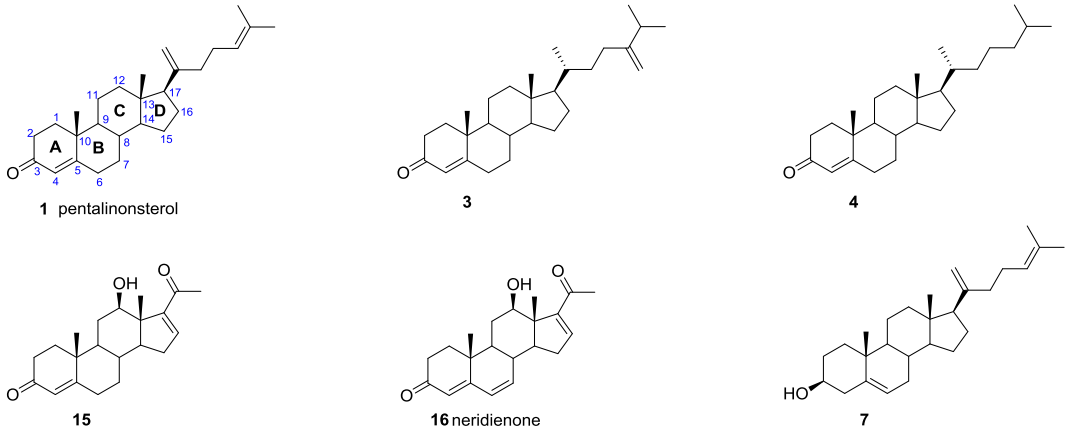

Figure 6 Structures of the most active compounds isolated from the roots of *Pentalinon Andrieuxii*.

Compound	*L. mexicana*	
	Promastigotes[b]	Amastigotes[c]
Cholestra-4,20,24-trien-3-one (**1**)	30.0	3.3
24-Methylcholesta-4,24(28)-dien-3-one (**3**)	24.0	3.5
Cholest-4-en-3-one (**4**)	81.0	0.03
Cholest-5,20,24-trien-3β-ol (**7**)	>262	14.5
6,7-Dihydroneridienone (**15**)	9.2	1.4
Neridienone (**16**)	26.2	3.5
Pentostam[d]	346.1	2.7

[a] Compounds with IC_{50} > 100 μg/mL are considered to be inactive.
[b] Results are expressed as IC_{50} values (μM), calculated by linear regression analysis from the K_C values at the concentrations used (1, 10, 50 and 100 μg/mL) at 48 h culture.
[c] IC_{50} for *L. mexicana* in bone marrow-derived macrophages from C57BL/6 mice (48 h experiment ran in triplicate).
[d] Used as a positive control substance.

Table 1 In vitro antileishmanial activities of compounds isolated from the roots of *Pentalinon Andrieuxii*[10]

It is also important to note that these compounds were also tested against uninfected mouse cells lines and showed no cytotoxicity, demonstrating a lack of toxicity to healthy tissue and selectivity for infected cells lines[10]. Analysis of **Table 1** shows us that, against amastigotes, compound **4** is the most active with an IC_{50} of 30 nM[10]. This compound is simply an oxidized derivative of cholesterol. All of the active compounds tested had similar activity to the pentostam control except compound **7**. This is important because these compounds have similar toxicity while being selective towards the infected cells. Examination of the antileishmanial activities and chemical structures of the isolated compounds provided a preliminary hypothesis for which chemical moieties are required for activity (pharmacophore determination). For example, the only difference between compounds **1** and **7** is the oxidation of the A-ring and based on the dramatic difference in potency, it can be hypothesized that the A-ring α,β-unsaturated ketone is important. However, while compound **7** lacks the A-ring oxidation, it is still relatively active. This is likely due to the presence of the same C17 side chain that is found in pentalinonsterol (PEN). Pentalinonsterol was one of two novel compounds isolated by the Kinghorn lab during this study, although it was the only one found to possess antileishmanial activity[10]. Unfortunately, only 1.2 mg of pure pentalinonsterol could be isolated from 900g of dried *P. Adrieuxii* roots, thus limiting biological studies of this compound. Based on the limited availability of the compound, structural novelty, and predicted relative ease of synthetic access to pentalinonsterol, a synthetic approach was developed in order to generate more pentalinonsterol for biological and mechanism of action studies and to determine the structure activity relationship of the chemical moieties of this natural product.

The Semi-Synthesis and optimization of Pentalinonsterol

Based on the need for a synthetic route to pentalinonsterol, a relatively simple synthetic scheme was devised starting from an inexpensive commercially available sterol (pregnenolone, $4.56/gram). The key reaction was proposed to be an enolate alkylation reaction which would install a prenyl unit onto the methyl ketone at the C17 position. The scheme below depicts the two closely related synthetic schemes that have been used to prepare pentalinonsterol. In **Scheme 1**, the initially reported procedures and yields of Dr. Dalia Abdelhamid, a former graduate student in the Fuchs lab, are enclosed in black boxes. Dr. Abdelhamid's route to pentalinonsterol provided the natural product in 25% overall yield from the starting pregnenolone[11] and demonstrated that the methyl ketone could be efficiently functionalized. Optimization of the synthetic route in collaboration with Mr. Andrew Huntsman, another undergraduate researcher in the Fuchs lab, led to the improved conditions reported in red. The optimized synthetic route was designed to increase the overall efficiency of the synthesis by increasing overall reaction yields as well as using less expensive reagents. Notably, this route increased the overall yield to nearly 50% and eliminated the use of the expensive and somewhat reactive Tebbe reagent.

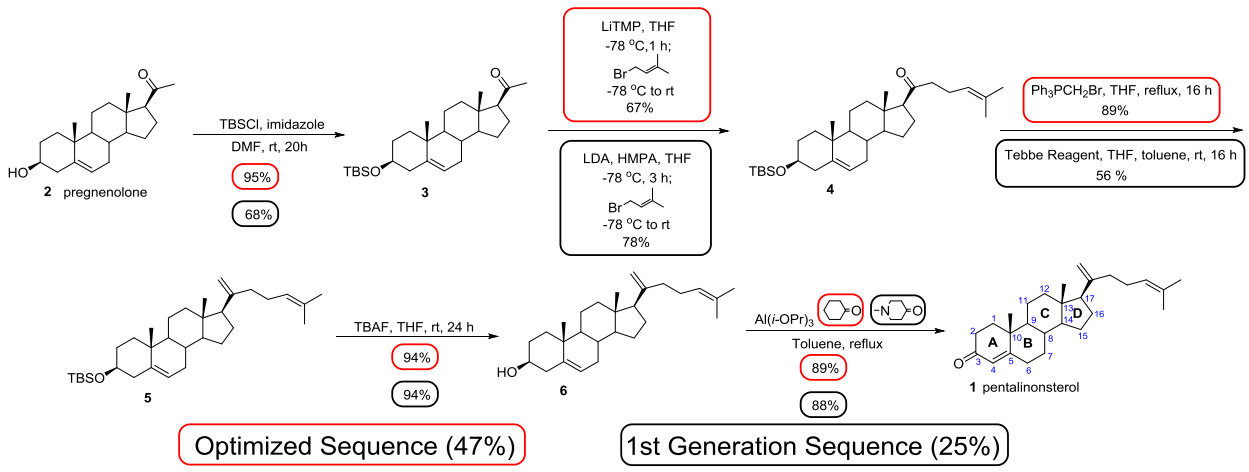

Scheme 1 The first and second generations of the semi-synthesis of pentalinonsterol

In both routes, the synthesis began with protection of the C3 alcohol of pregnenolone. This protection reaction was run under the same conditions in both cases, although upon repeating the reaction on larger scale a 94% yield of the protected pregnenolone could be obtained as a precipitate. In these syntheses, TBSCl is used as the protecting agent instead of the more commonly employed acetate group in order to provide increased stability in the subsequent alkylation reaction.

Precedented procedure for the alkylation on the C21 position of pregnenolone through the kinetic enolate formation was reported by Hanson *et. al.*[12]. We chose to use strong, sterically hindered bases in order to generate the kinetic enolate which was then alkylated upon addition of the 3,3-dimethylallyl bromide. Dr. Abdelhamid used LDA to form the kinetic enolate and HMPA as a cosolvent to make a more reactive "naked" enolate. Attempts to reproduce this result for the revised synthesis failed to produce the same yield of product. As an alternative, LiTMP was utilized in place of LDA and HMPA in order to achieve our highest yield of 67%. Utilization of LiTMP allowed us to avoid the distillation and use of the highly carcinogenic HMPA. Another key change to Dr. Abdelhamid's procedure was a change in the purification technique. Due to the lipophilicity of the alkylated product, she employed gravity columns with very non-polar systems. In order to optimize this process, we found that a gradient column run from 0 EtOAc: 0 DCM: 100 Hexanes up to 2:2:96 allowed us to separate the desired monoalkylated product from the undesired dialkylated product as well as the starting material while using flash column chromatography methods. Ultimately, variations in the yields of these alkylation reactions were observed, and were attributed to the quality of the reagents, the scale on which the reaction was run, and attention to laboratory techniques for the handling of air- (or water-) sensitive materials.

With the alkylation adduct in hand, the next task involved the olefination of the carbonyl in the C17 side chain. Dr. Abdelhamid used the highly reactive Tebbe reagent in order to effect olefination of this ketone. Although the yield of the reaction was acceptable, the Tebbe reagent is rather expensive ($58.61/gram) and was found to degrade rapidly upon storage. In addition, workup of this reaction resulted in an emulsion which made the extraction extremely time consuming. In the revised synthesis, it was found that the olefinated product **5** could be effectively generated through Wittig olefination, which is much cheaper than the Tebbe reagent. This modification required the use of excess Wittig reagent ($1.01/gram), but provided much higher yields of the desired product.

After the fully functionalized C17 side chain had been installed, all that remained to do was the deprotection of the TBS ether and subsequent oxidation of the sterol A-ring. The TBAF deprotection of the alcohol was done as previously reported with similar yield. Dr. Abdelhamid initially employed a well-precedented Oppenauer oxidation with cyclohexanone as the co-oxidant in an attempt to generate the natural product. She reported, however, that under these conditions a mixture of oxidized products, including the ketone product in which the B-ring olefin did not undergo isomerization to the α,β-unsaturated ketone, were generated. Based on this result, she switched to the higher boiling 1-methyl-4-piperidone which had previously been reported by Keana *et. al*[13]. During optimization it was determined that cyclohexanone could be used effectively in this transformation. We believe that the isomerization issue was avoided because the reaction was run overnight. This increased reaction time would allow more time for formation of the thermodynamic product. Employing the optimized synthetic sequence, pentalinonsterol was generated on gram scale.

Proposed Mechanisms of Action of Pentalinonsterol

As anticipated, the synthesis of pentalinonsterol has facilitated further biological testing of this natural product. In the original isolation paper, the authors demonstrated that the natural product had promising antileishmanial activity, but the exact nature of this activity was unknown. It was postulated that the sterol compounds may act as antagonists of endogenous biosynthetic pathways for leishmanial sterols[10], although other hypotheses also included interaction with or destabilization of the membrane and effects on the host immune system.

Biological testing performed by the Parinandi lab at the Ohio State University has shown that treatment of *L. donovani* promastigotes with PEN led to a decrease in the saturated and unsaturated fatty acid composition in the lipids which can be seen in **figure 7**. This is proposed to effect phospholipases A_1 and A_2 via a hydrolysis and metabolomics breakdown of the fatty acid esters in the membrane of the parasites[14]. Alteration of the fatty acid content in the lipid bilayer could make the membrane more porous and result in leaking of cellular components, resulting in cell death. PEN has potential efficacy against multiple Leishmania species since the fatty acid content among all of the known species of Leishmania is consistent[14].

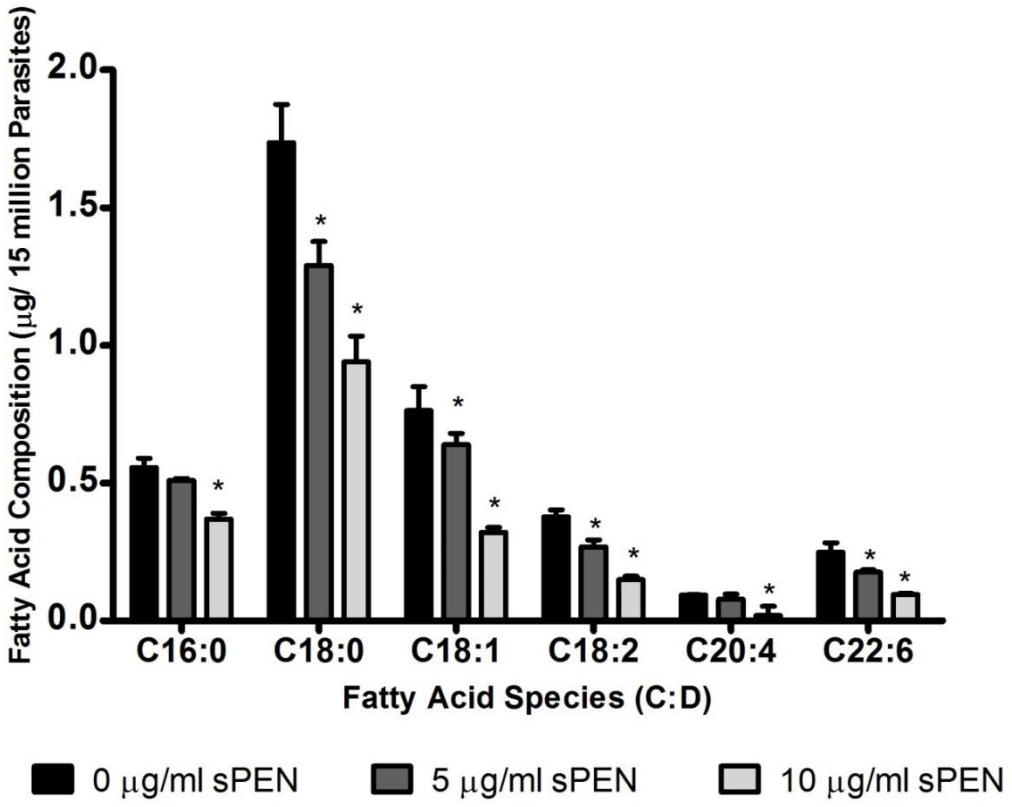

Figure 7 Fatty acid disruption in *Leishmania donovani* promastigotes by sPEN. Fatty acid composition of *L. donovani* promastigotes treated with or without sPEN (5 and 10 µg/ml) for 12h. Fatty acids in total membrane lipids were derivatized into methyl esters by alkaline methanolysis and analyzed by gas chromatography-mass spectrometry. C16:0 = palmitic acid; C18:0 = stearic acid; C18:1 = oleic acid; C18:2 = linoleic acid; C20:4 = arachidonic acid; C22:6 = docosahexaenoic acid. Data are presented as mean of three replicates ±S.D. Statistical significance with respect to 0 µg/ml sPEN is presented as *$p < 0.05$[14].

The Satoskar lab has also reported PEN to be more effective at treating intracellular amastigotes than promastigotes. This is ideal because the infected hosts contain the amastigote form of the leishmaniasis which is the form that is actively being treated. It is also important to remember that PEN is not cytotoxic towards healthy host macrophages making this a clinically relevant drug. Due to PEN's poor water solubility due to its extremely high lipophilicity the Ainsley lab at the University of North Carolina has a liposomal formulation of PEN that allows it to be administered and used for *in vivo* testing. When using liposomal PEN (lPEN) to treat infected mice, a significantly lower parasite load was seen in the liver, spleen, and bone marrow **(figure 8)**.

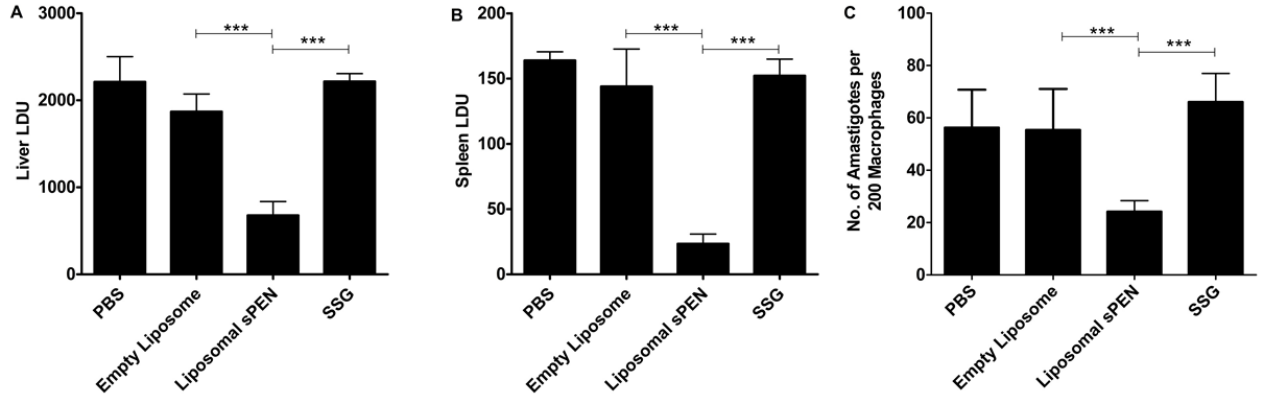

Figure 8 Liposomal sPEN treatment renders protection against *L. donovani* infected mice. (A) Liver (B) spleen and (C) bone marrow parasite loads in *L. donovani* infected BALB/c mice treated with either PBS, empty liposomes, sPEN loaded liposomes (50 µg or 2.5 mg per kg body weight), or sodium stibogluconate SSG (70 mg per kg body weight). Parasite burdens in spleen and liver were expressed as mean LDU; parasite burden in bone marrow was expressed as number of amastigotes per 200 macrophages. Data is presented as mean ± SE. These data are mean values from four or five individual mice per group at each time point in three independent experiments with similar results. Significance is presented as *** p < 0.001[14].

In conjunction with parasite load reduction, it has been observed that PEN may also act as an adjuvant. Not only does PEN reduce parasite load, but it also is thought to enhance the lympho-proliferative responses in the host. After treatment with lPEN, infected mice showed an increase in T cell proliferation. This is important because active VL impairs the immune response preventimg the T cells from responding to the infection properly. Treatment of the mice with lPEN also increased the production of IFN-γ[14] which is a cytokine that is responsible for inate and adaptive immunity against infections (**figure 9)**. It has been proven that IFN-γ is responsible for clearance of leishmaniasis from infected cells[15] which is why it is beneficial that PEN can increase these levels. In conclusion, PEN is capable of killing leishmaniasis via two mechanisms, alteration of the fatty acid content in the parasites lipid bilayer and enhancing a protecting immune respone by increasing IFN-γ levels leads to eradication of the leishmaniasis[14].

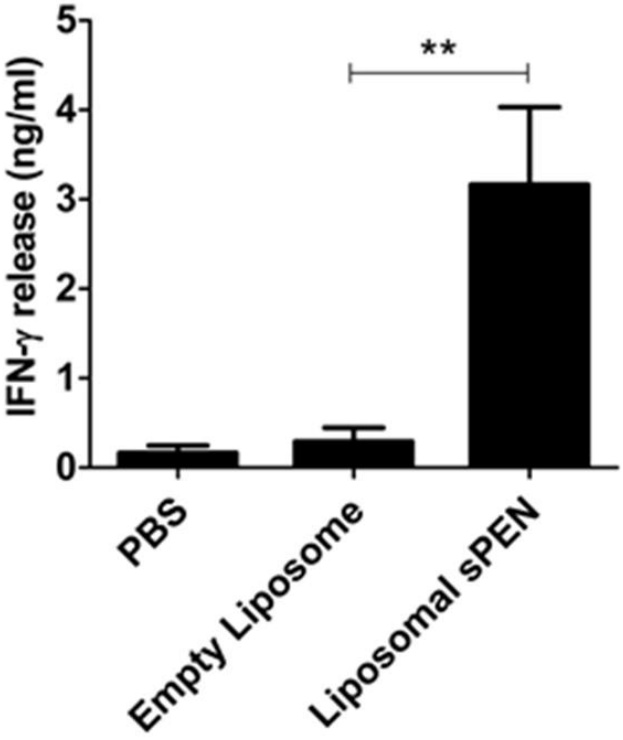

Figure 9 IFN-γ levels in infected mice cells after treatment with lPEN

Structural Derivatives of Pentalinonsterol as Mechanistic Probes

With an established synthetic route to pentalinonsterol, structural derivatives of the compound were pursued for Structure Activity Relationship studies (SAR). The approach to analogue generation targeted the key α,β-unsaturated ketone of the A-ring and the C17 side chain moiety. A-ring analogues were synthesized by Mr. Andrew Huntsman while my role involved the synthesis of the C17 side chain analogues.

Figure 10 A list of the alkyating agents used to make pentalinonsterol derivatives

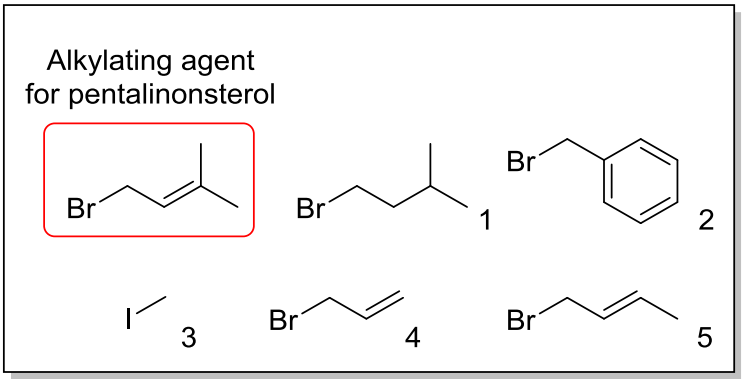

The first task required for derivatization of the C17 chain was to determine what electrophiles would be tolerated in the alkylation reaction. **Figure 10** lists the different alkylating agents that were used in order to create new side chain analogues. The alkylation reaction was carried out using the procedure optimized for the preparation of pentalinonsterol, namely enolate generation with LiTMP followed by addition of the appropriate alkyl halide. After successful alkylation, the synthesis would be continued in the same manner employed for the preparation of pentalinonsterol. The key difference in the synthetic sequences was the re-evaluation of the solvent systems that needed to be used for flash column chromatography. Due to the extreme lipophilicty of these molecules, multiple solvent systems had to be tested and optimized for each alkylated and olefinated products. The most difficult purifications were those of the alkylation products themselves due to the similar polarities between the mono and dialkylated products. In

order to achieve minimal coelution, the solvent polarity employed for flash column chromatography typically had to be reduced, resulting in much slower elution of the compounds.

In order to understand why the alkylating agents were chosen it is important to compare their structures to that of dimethylallyl bromide. Reagent 1 is the saturated form of dimethylallyl bromide and closely resembles cholesterol. Reagent 2 was chosen to see if adding an aromatic substituent in place of the prenyl group would increase activity through potential π-π interactions. Reagent 3 was chosen in order to probe the importance of the C17 chain length. Reagents 4 and 5 allow us to probe the importance of the dimethyl portion of the prenyl group.

As mentioned above, the electrophiles that could be tolerated in the alkylation reaction had to be probed. Only three of the alkylating agents seen in **figure 10** were determined to be suitable electrophiles. Reagents 2, 3, and 4 alkylated successfully with yields of 55, 68, and 44% respectively. Most notably, only the most reactive alkylating agents were suitable for this reaction, possibly due to the relatively congested steric environment of the methyl ketone. It was surprising to see that reagent 5 was unable to be successfully alkylated to the sterol since it has similar reactivity to reagents 2, 4, and dimethylallyl bromide (other allylic or benzylic halides) which all alkylated successfully. The consideration of electrophile reactivity helps to explain why reagent 1 could not be successfully employed. Experiments are currently being performed to increase reagents 1's electrophilicity by converting the bromine to a better leaving group. A Finkelstein reaction was attempted on this material with NaI, however, only starting material was recovered. Other reactions can be employed such as triflation, although care must be taken not to introduce a leaving group that will subsequently eliminate.

Upon each successful alkylation reaction, new chromatographic solvent systems were required to successfully separate the products given that the lipophilicty was different. However,

once pure alkylated product was isolated the synthesis was continued in the same manner employed for the preparation of pentalinonsterol. Compounds RD36, RD50, and RD51 were successfully completed and submitted for biological testing. RD50 is unique because the olefination step was omitted in order to probe the importance of the side chains olefin.

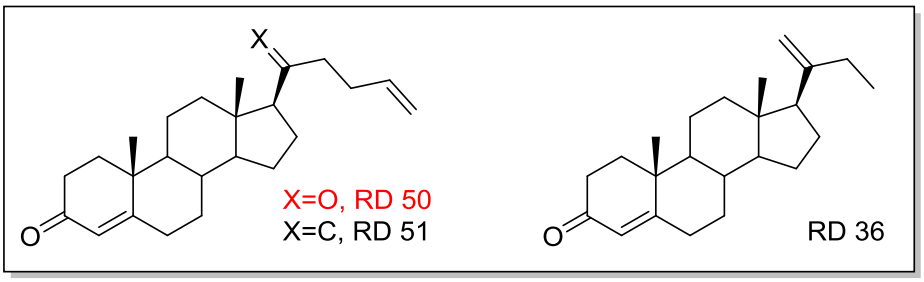

Despite successful alkylation with benzyl bromide, isolation of the final analogue in this case was prevented by contamination issues. Triphenylphosphine was discovered in the ^{1}H NMR and was found to be inseparable from the olefinated product. Trituration with hexanes was employed to remove the triphenylphosphine as seen in the NMR spectra in **figures 11** and **12**, however this derivative was soluble in hexanes so we could not purify this intermediate until the silyl ether deprotection. Another similar analogue was attempted where the olefination step was omitted, however this sample was contaminated with plasticizer. After multiple purification attempts with multiple solvent systems the impurities were still present in the sample as seen in **figure 13**. It is possible that these impurities could have been removed after the subsequent deprotection step, but due to multiple attempts at purification, the quantities of compound remaining were not sufficient to take forward in the synthesis.

Figure 11 Triphenylphosphine impurity after olefination

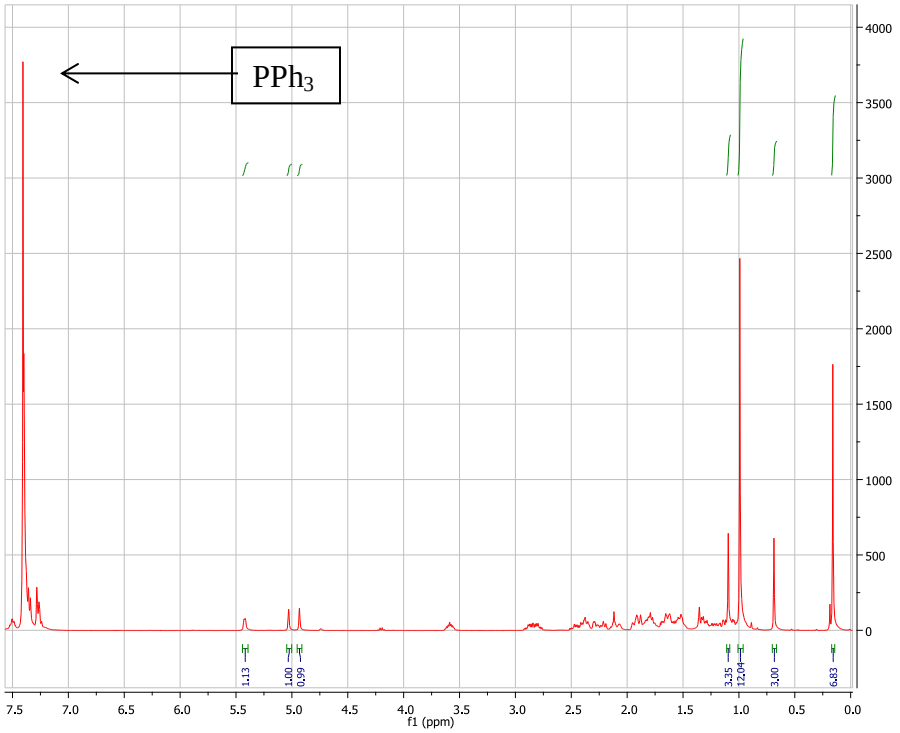

Figure 12 Enhanced view of the PPh_3 impurity

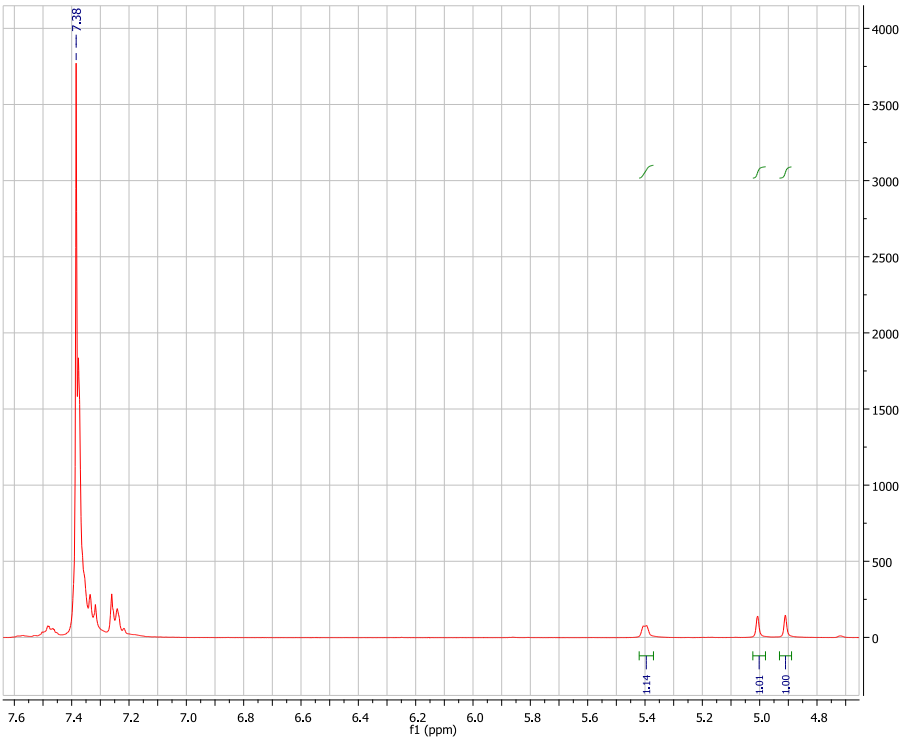

Figure 13 Display of the unknown impurities after the Oppenauer oxidation

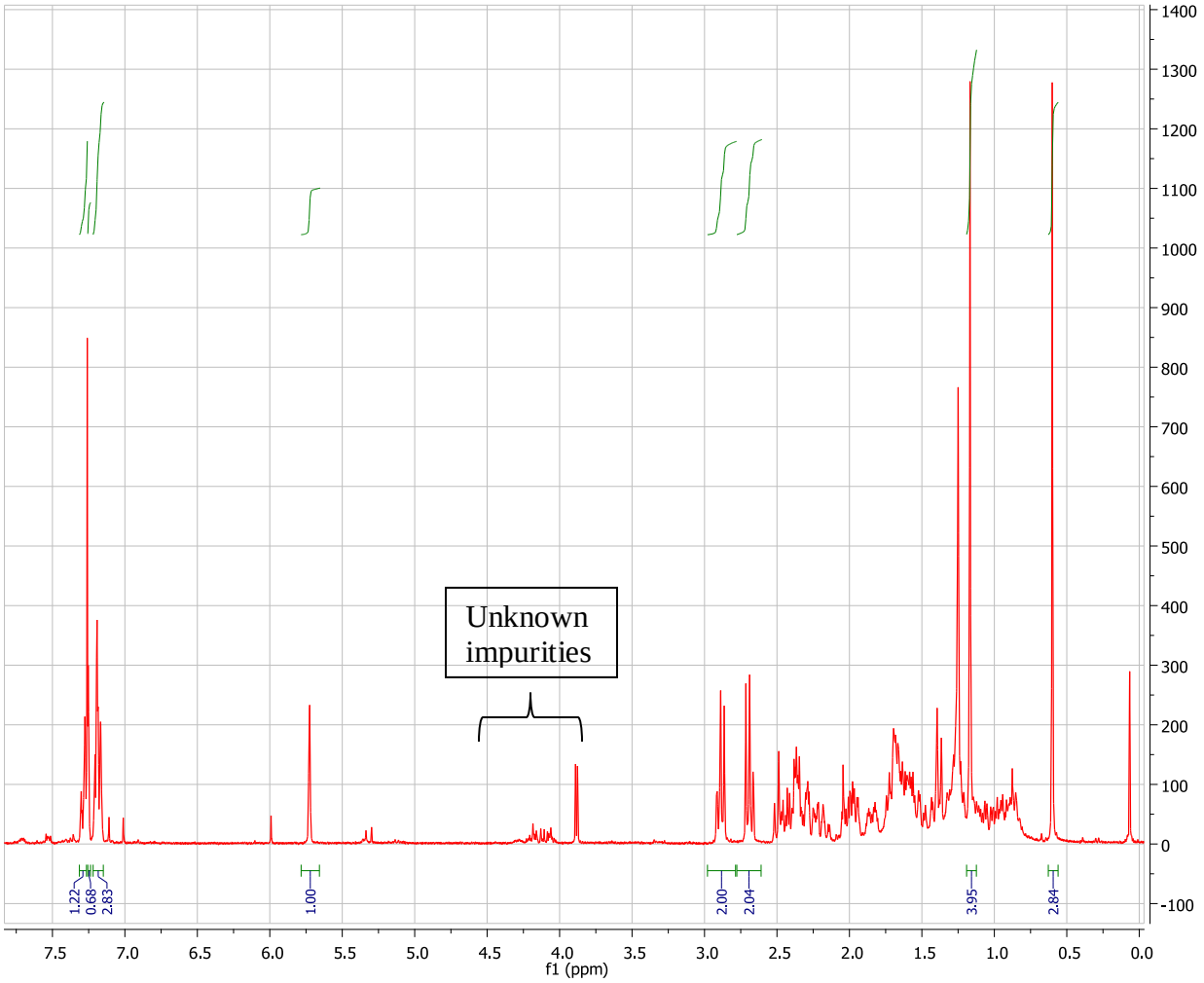

Compounds 4 and 5 were never completed due to poor reactivity of alkylating agents 1 and 5. Since analogues were needed for biological testing the synthesis of these compounds was de-prioritized and temporarily put on hold. The issue of sterol alkylation may be readdressed in future works.

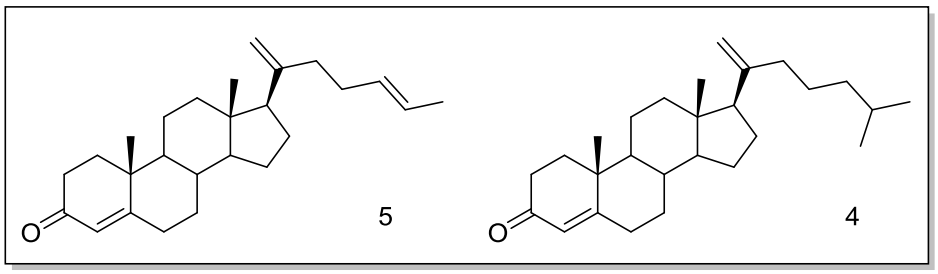

Figure 14 Structures of the analogues sent for biological testing

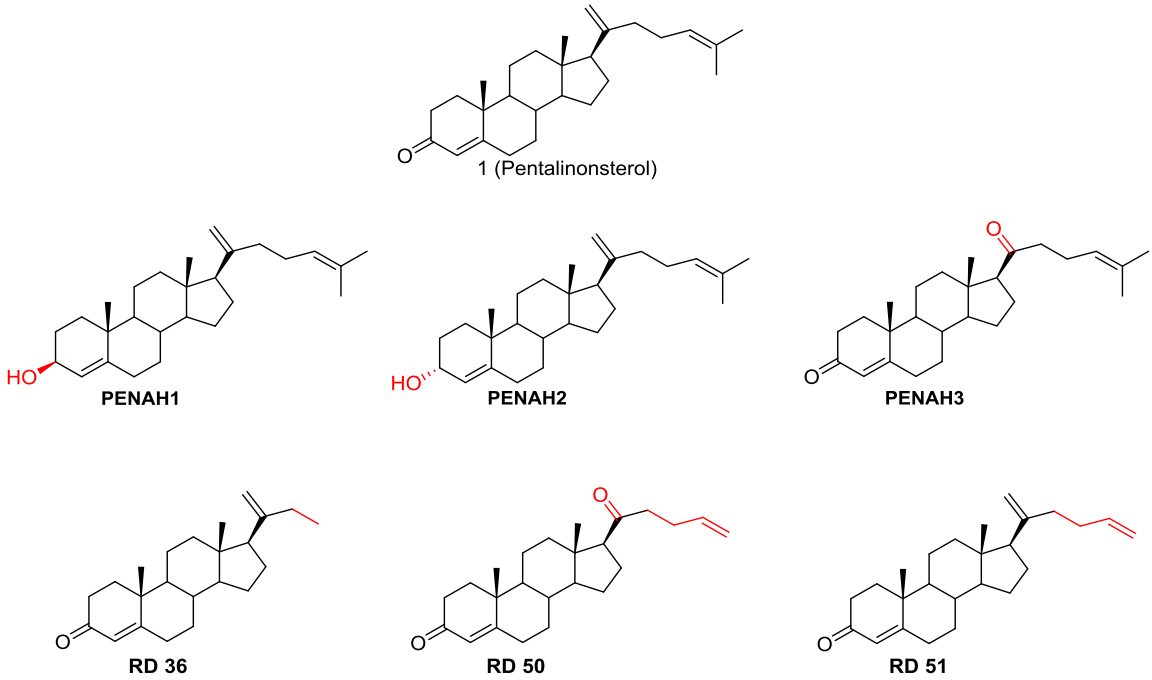

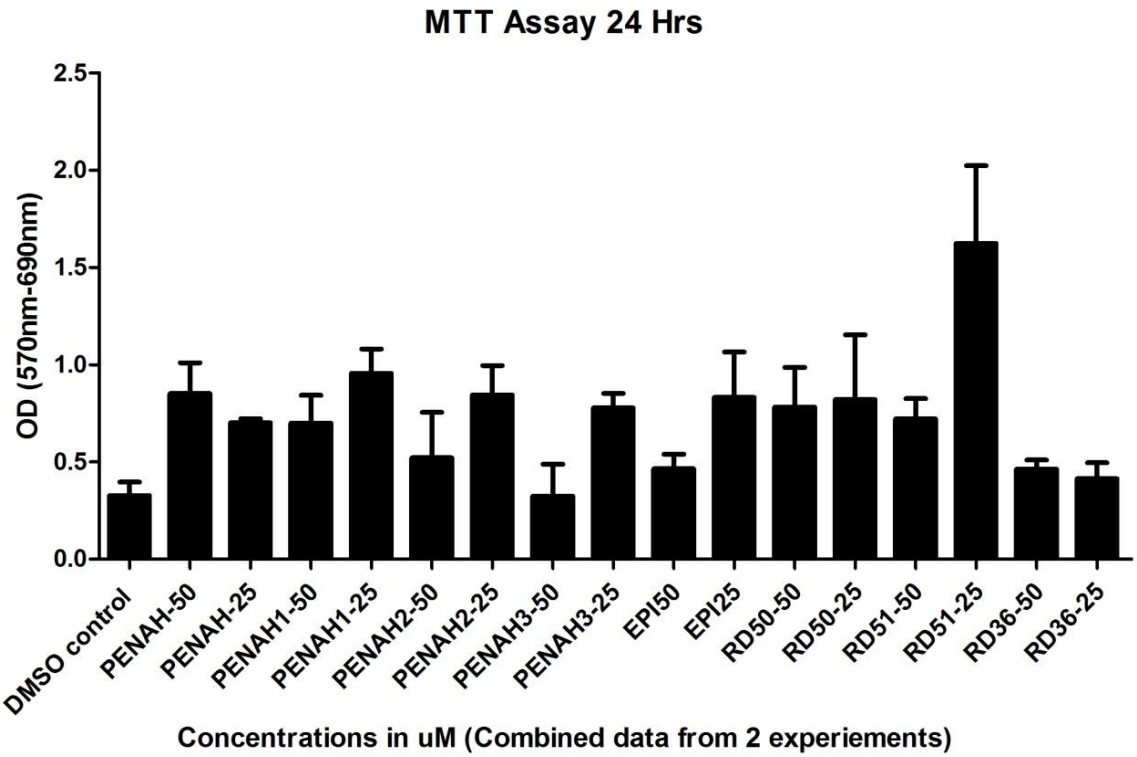

Figure 15 Compounds tested in an MTT assay to determine the cytotoxicity against healthy dendritic cells

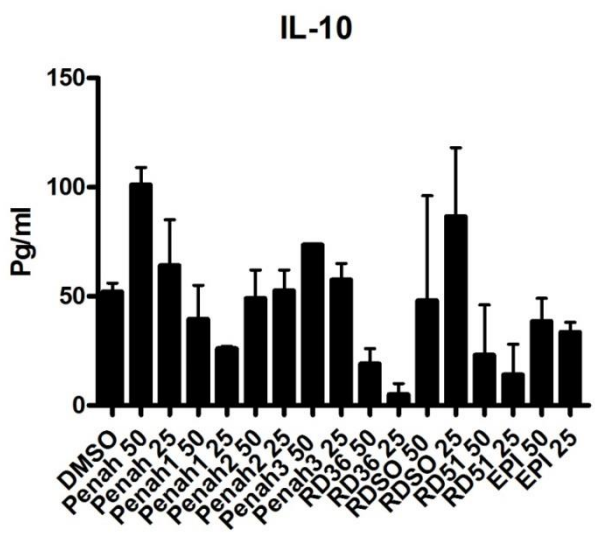

Figure 17 PEN analogues were tested to see their effects on IL-10 levels.

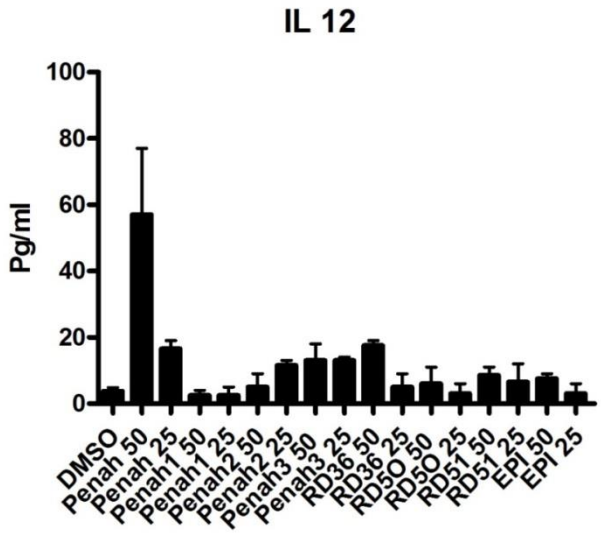

Figure 16 PEN analogues were tested to see their effects on IL-12 levels

The Biological Activity of Pentalinonsterol Derivatives

In order to probe the activity of each analogue it is important to compare the relative potency to PEN itself. Biological testing of the compounds highlighted in **figure 14** were done in the Satoskar lab, and the results are displayed in **figures 15-17**.

The first test that was performed on the analogues was an MTT assay. An MTT assay is a colorimetric assay that tests cell viability. In this assay the MTT (3-(4,5-dimethylthiazol-2-yl)-2,5-diphenyltetrazolium) tetrazolium dye is added to each well in a well plate with healthy dendritic cells (DC's). Each well is then dosed with a different concentration (25 or 50 μM) of the analogues and then after 24 hours the color of the wells is recorded as an optical density which correlates to the amount of living cells. The MTT is reduced enzymatically by oxidoreductase in the living cells to the insoluble formazan which has a purple color. This means that wells that have more purple color will have a higher optical density which corresponds to more cell proliferation.

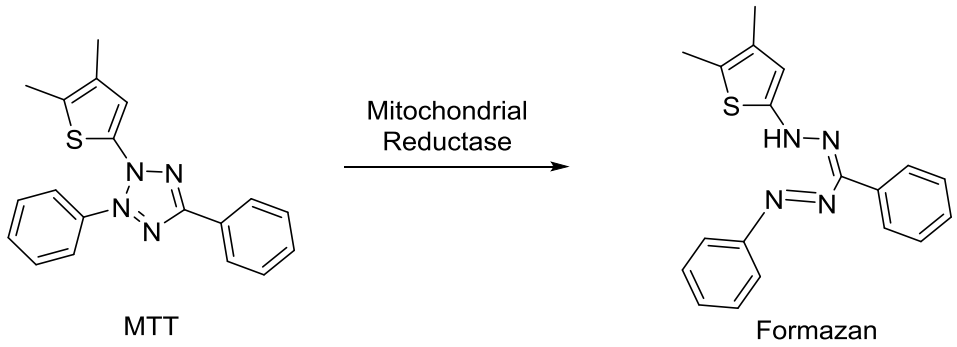

Figure 18 The reduction of colorless MTT to the purple Formazan *in vivo*.

Analysis of the MTT assay data shows that all of the compounds are not toxic to the DC's when compared to DMSO. It is important to note that DMSO itself is a relatively non-toxic compound that is frequently used as a carrier for *in vitro* and *in vivo* testing. DMSO is most commonly used as a solvent to dissolve hydrophobic drugs for this type of assay and is also used for cryopreservation of compounds. It has been employed in multiple different models[16].

Analysis of **figures 16** and **17** shows that all of the analogues that were tested were not as effective as PEN at increasing IL-12 levels but were equally or more effective at decreasing the IL-10 levels. Since IL-12 is responsible for IFN-γ production, it is optimal to show an increase in IL-12 levels[14]. While none of the analogues were as effective as PEN, RD36 at 50 μM was the most effective at increasing these levels. Since IL-10 is responsible for inhibition of IL-12 it is ideal to see a decrease in IL-10 levels[17]. Compounds RD36 and RD51 seemed to be the most effective at inhibiting the production of IL 10.

Future Works

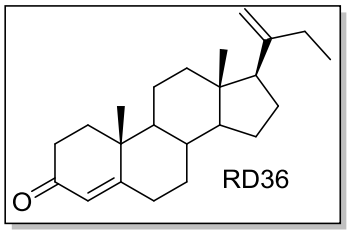

The Satoskar Lab is currently in the process of generating antileishmaial activity data for the submitted compounds. This data will be critical for further optimization of the compounds. This will also help to determine the role and function of the side chain. Currently it appears that RD36 seems to be the most promising compound with regard to adjuvant activity. It is possible that adjuvant and antileishmanial activity could be optimized in these compounds concurrently or separately depending on the potential application.

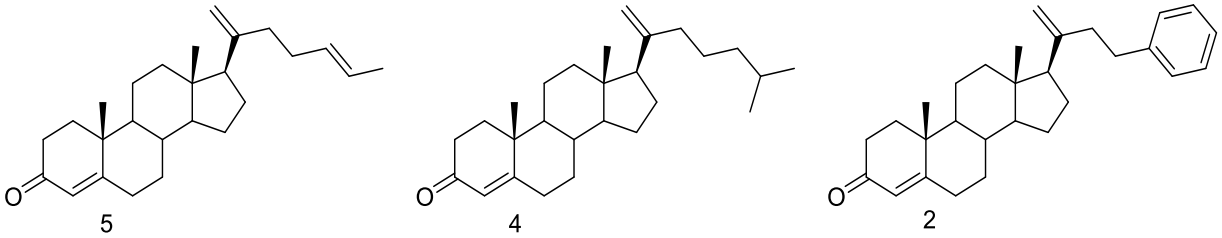

Figure 19 Remaining compounds to be synthesized to complete the analogue library

In order to complete the analogue series we will ultimately want to go back and finish the synthesis of the molecules that are shown in **figure 19.** These compounds will allow us to fully understand the importance of the prenyl side chain that is found on PEN. The synthesis of compound **2** can be accomplished utilizing the procedure that was developed. In this case, however, more care will have to be taken in order to prevent the introduction or production of impurities in the synthesis. We believe that the alkylation issues that we have encountered in the synthesis of compound **5** can be overcome since the alkylation reagent has similar reactivity to other reagents that have been employed successfully. We may need to use HMPA in combination with the LiTMP In order to make a more "naked" and reactive enolate. Switching the solvent to a more polar aprotic solvent may increase reactivity through stabilization of the

intermediate of the SN2 reaction however solubility issues may arise if the solvent becomes too polar. It was mentioned earlier that compound **4** might be able to be made if we can modify the leaving group. Introduction of a triflate group on the electrophile will increase its reactivity, although we must be careful because as better leaving groups are introduced the risk of elimination before the molecule reacts increases.

Part II: The Total Synthesis of Scytonemide A, a Novel 20S Proteasome Inhibitor

Chapter 1: The Ubiquitin Proteasome Pathway and Its Inhibitors

The Ubiquitin Proteasome Pathway

The ubiquitin proteasome pathway (UPP) is responsible for the degradation of intracellular proteins. The system is capable of degrading proteins from the nucleus, cytosol, membrane anchored, and secretory pathway-compartmentalized proteins[18]. Due to the vast array of cellular targets that this pathway can affect, the UPP is responsible for regulation of cell cycle and division, neuronal works, ion channels, DNA repair, regulation of immune and inflammatory response, development and differentiation, and apoptosis[18]. Due to the multifaceted purpose of the UPP its regulation is critical to cell vitality and viability.

Degradation of cellular proteins can be broken down into two successive steps which are displayed in **figure 20**. The first step involves the covalent polyubiquitination of single ubiquitin units to the protein that is to be degraded. The ubiquitination process is driven by three key enzymes. Ubiquitin activating enzyme (E1) activates the C-terminal glycine of a single ubiquitin molecule which becomes coordinated to an ubiquitin-protein ligase enzyme (E3) by the ubiquitin conjugating enzyme (E2). E3 is the enzyme that covalently links ubiquitin to a lysine residue of the protein. Once the protein is polyubiquitinated, through subsequent ubiquitination of lysine residues of the previous ubiquitin molecule, it becomes recognized by the proteasome.

The 26S proteasome is responsible for the degradation of polyubiquitinated proteins and it can be broken down into two subunits: The 20S proteasome, which is responsible for the catalytic degradation of proteins, and the two flanking 19S subunits which recognize the polyubiquitinated proteins. It is currently theorized that entry of the protein into the catalytic 20S core does not take place until the 19S subunit undergoes a conformational change which opens up a pore. Once the protein enters the 20S proteasome it is degraded by trypsin, chymotrypsin, or post-glutamyl peptidase sites.

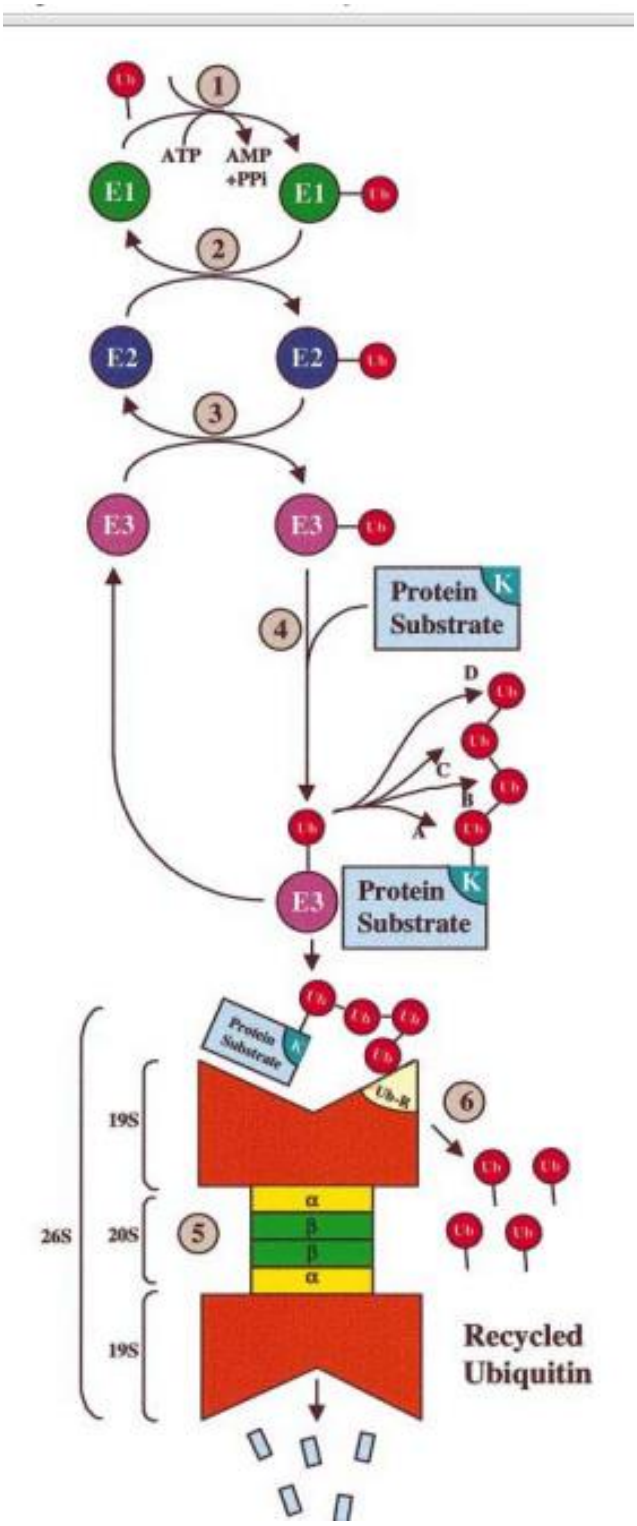

Figure 20 The Ubiquitin Proteasome Pathway[18]

UPP Inhibitors

Due to the UPP's involvement in the degradation of over 80% of cellular proteins[19] it can be understood why defects in this pathway can have dire consequences on cellular health. The first proteasome inhibitors were developed as mechanistic probes in order to understand the function of the 20S proteasome. Initial inhibitors lacked specificity, potency, or availability[19]; however significant improvements have been made. Recent biological studies have demonstrated that proteasome inhibitors are more cytotoxic towards malignant cells than healthy cells, although the exact reason for this is still undetermined. It is believed that the highly proliferative tumor cells have increased protein synthesis rates and inhibiting the proteolysis of key proteins can lead to apoptosis. It is well understood that the cellular cycle is tightly controlled through cyclins and cyclin dependent kinases (CPK's) and loss of control of this system can lead to oncogenesis[19]. The UPP is responsible for the degradation of many of the proteins that are critical for cellular regulation. If proteasome inhibitors successfully inhibit the proteolysis of cyclins or specific regulatory proteins then the cell undergoes induced cell death via cell cycle arrest[19]. The UPP is also responsible for the degradation of intracellular pro and anti-apoptotic proteins. Inhibition of the proteasome results in the upregulation of proapoptotic factors while reducing the levels of antiapoptotic factors. This results in apoptosis in cancer cells that have disregulated levels of these factors. It has been proven that the proteasome inhibitors can be used as an effective single component treatment or they can be used in conjunction with other chemotherapeutics to increase their efficacy[19]. Three major classes of proteasome inhibitors have or are currently being developed for clinical use. There are peptide boronic acids, peptide epoxyketones, and β-lactones which bind either reversibly or irreversibly to the catalytic site of the 20S proteasome.

Bortezomib

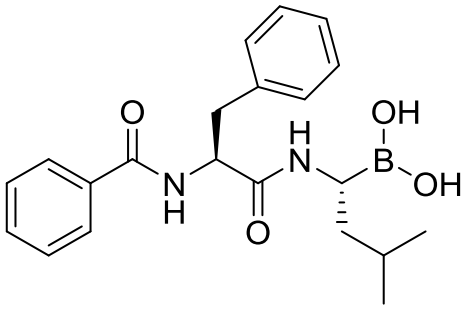

Bortezomib is a reversible 20S proteasome inhibitor. This drug appeared to be most effective against multiple myeloma and was first approved by the FDA as a third-line treatment in 2003. The drug became a first-line treatment in 2008 for multiple myeloma. It is mainly used in tandem with other chemotherapeutic agents in order to overcome resistance and sensitivity issues. A major setback with Bortezomib is its inability to effectively treat solid tumors. The drug showed promise in preclinical studies but failed to perform in clinical trials. This limitation has opened the door for broader spectrum proteasome inhibitors[19].

Carfilzomib

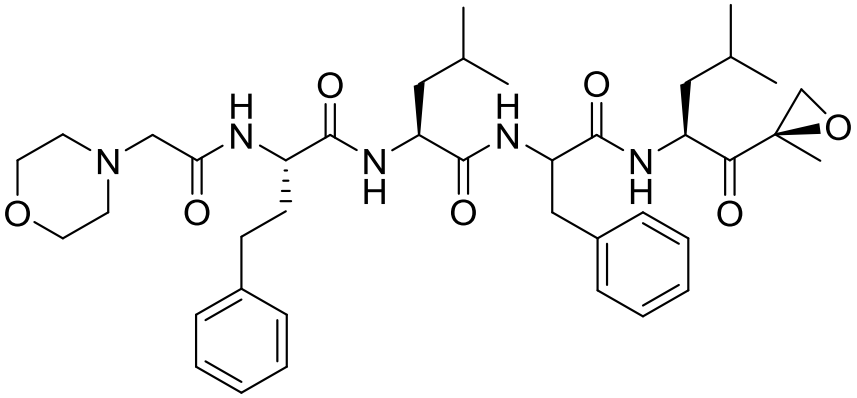

Carfilzomib is a member of the epoxyketone family of proteasome inhibitors and binds to the catalytic site of the 20S proteasome at two different sites. The drug binds irreversibly to both

the amino and hydroxyl groups of the catalytic Threonine residue. Carfilzomib is shown to have similar potency to Bortezomib however this drug is more selective. This drug is also used with other chemotherapeutics for a synergistic effect[19]. Carfilzomib received FDA approval in July 2012 for the treatment of multiple myeloma in patients who have previously received other therapies, including Bortezomib.

Salinosporamide A

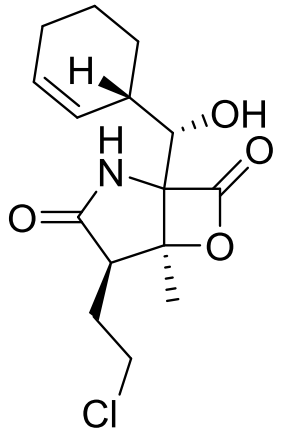

Salinosporamide A is a β-lactone proteasome inhibitor that is capable of binding to all 3 catalytic sites within the 20S proteasome. Another benefit of this drug over Bortezomib and Carfilzomib is its ability to be administered orally. This drug is also effective against Bortezomib resistant multiple myeloma cells lines[19].

MLN9708, CEP-18770, andONX0912

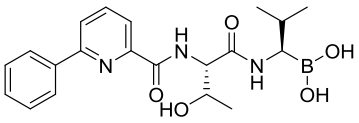

CEP-18770

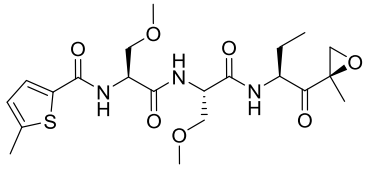

ONX 0912

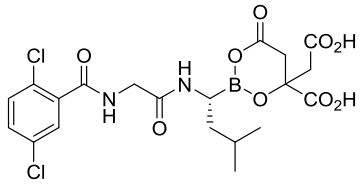

MLN9708

The remaining three proteasome inhibitors seen above are in the beginning of their clinical trials. CEP-18770 and MLN9708 are Bortezomib derivatives. MLN9708 has a significantly shorter half-life than Bortezomib which may increase its tissue distribution. It is also important to note that this compound is a prodrug that gets hydrolyzed to its biologically active form, MLN2238, *in vivo*. CEP-18770 shows improved cytotoxicity towards multiple myeloma cells while being less cytotoxic towards healthy cells. Compound ONX 0912 is an orally bioavailable version of Carfilzomib and is therefore more clinically desirable. All three of these compounds are in phase I or II of clinical trials[19].

Chapter 2: The Discovery and Approach Towards the Total Synthesis of Scytonemide A

The Discovery and Isolation of Scytonemide A

Natural products and their derivatives are responsible for 79.8% of all of the new anticancer drugs since 1981[9]. This number has actually risen over the past 10 years despite advances in combinatorial chemistry and high throughput screening. In order to discover new natural products with high proteasome inhibitory potency, researchers are looking towards natural sources such as plants and microorganisms. It is important to continue researching and discovering new proteasome inhibitors because there are only two FDA approved drugs and both of these have deleterious side effects or lack activity against certain types of tumors. With this in mind, cyanobacteria have been found to be an excellent source of multiple classes of secondary metabolites that have activity against many different diseases. As part of a collaborative research program project grant (P01) through the NIH, the Orjala lab at The University of Illinois Chicago employed bioassay-guided fractionation techniques on lyophilized *Scytonema hofmannii* in order to discover new novel 20S proteasomes inhibitors.

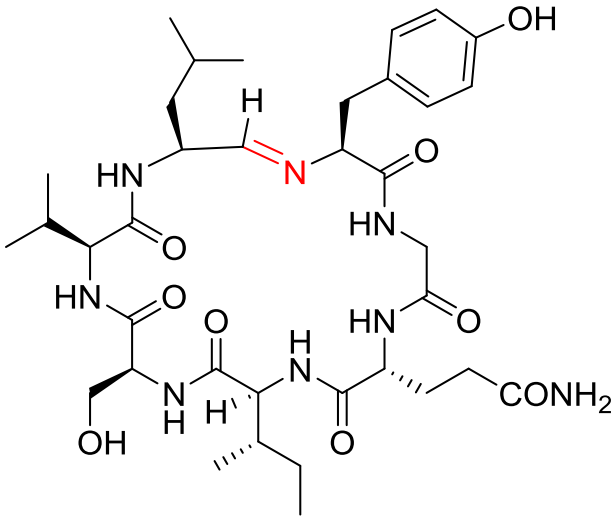

Figure 21 Scytonemide A

Scytonemide A, seen in **figure 21**, was reported to be a novel 20S proteasome inhibitor in the Orjala lab in 2010[20]. Two related compounds, Scytonemides A and B, were isolated from the 100% MeOH fraction, although only Scytonemide A showed potent inhibition of the 20S proteasome with an IC_{50} of 96 nM. While Scytonemide A showed promising *in vitro* proteasome activity (Table 1), it lacked activity in an HT-29 cell based assay. This was surprising because these cells have been shown to be sensitive towards proteasome inhibitors[20]. A luminescence based assay was used to ascertain the reason for the drastic decrease in activity and found that the poor result was due to the poor chemical or metabolomic stability of Scytonemide A. Scytonemide A showed activity at 6.7 µM in the luminescence based assay whereas it showed no activity at all in the HT-29 assay.

Compound	**Scytonemide A**
IC_{50} (20S Proteasome, chymotrypsic catalytic activity)	**96 nM**
ED_{50} (HT-29 cytotoxic assay)	**>20 µg/ml**
ED_{50} (luminescence based assay)	**6.7 µM**

Proposed Mechanism of Action

Scytonemide A contains a unique imine linkage which is highlighted in red in **figure 21**. This functionality is relatively unique for a cyclic peptide and is proposed to be responsible for its mode of inhibition. To understand why Scytonemide A acts as a 20S proteasome inhibitor it is important to understand how the clinically approved proteasome inhibitors work. The schemes below display the mechanisms of action for the 3 different classes of the clinically used

proteasome inhibitors as well as another proteasome inhibitor, fellutamide B, which has been shown to increase Nerve Growth Factor in cells[21].

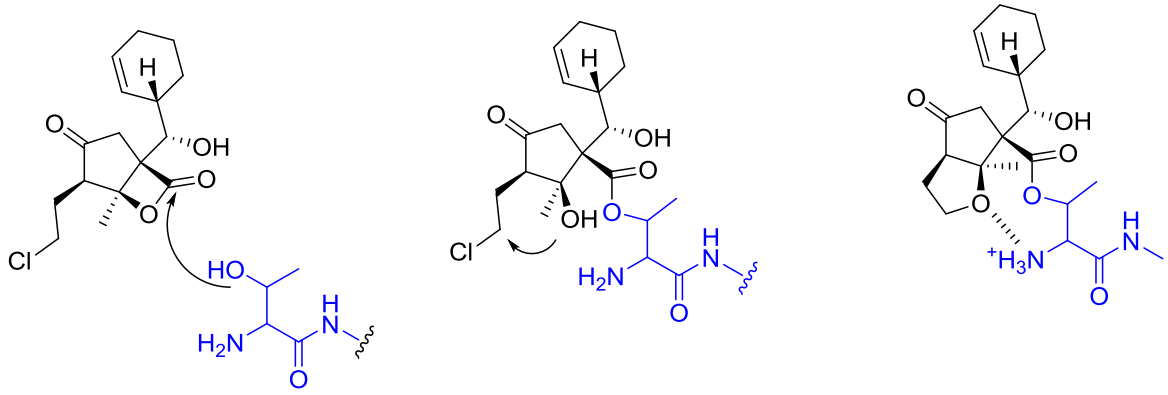

β-lactone inhibitor Mechanism (Salinosporamide A)

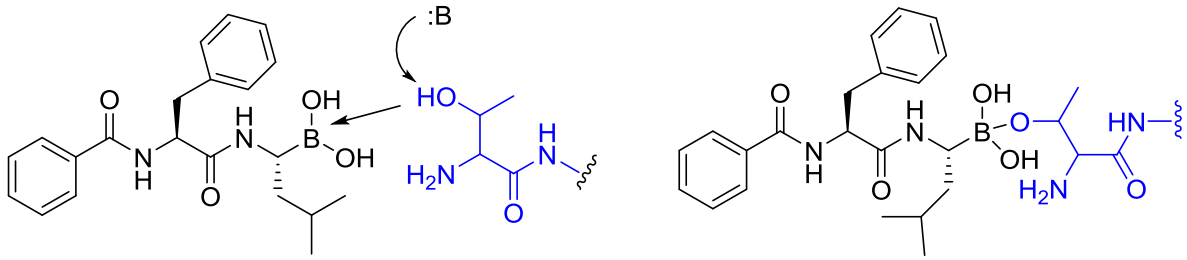

Boronic Acid Inhibitor Mechanism (Bortezomib)

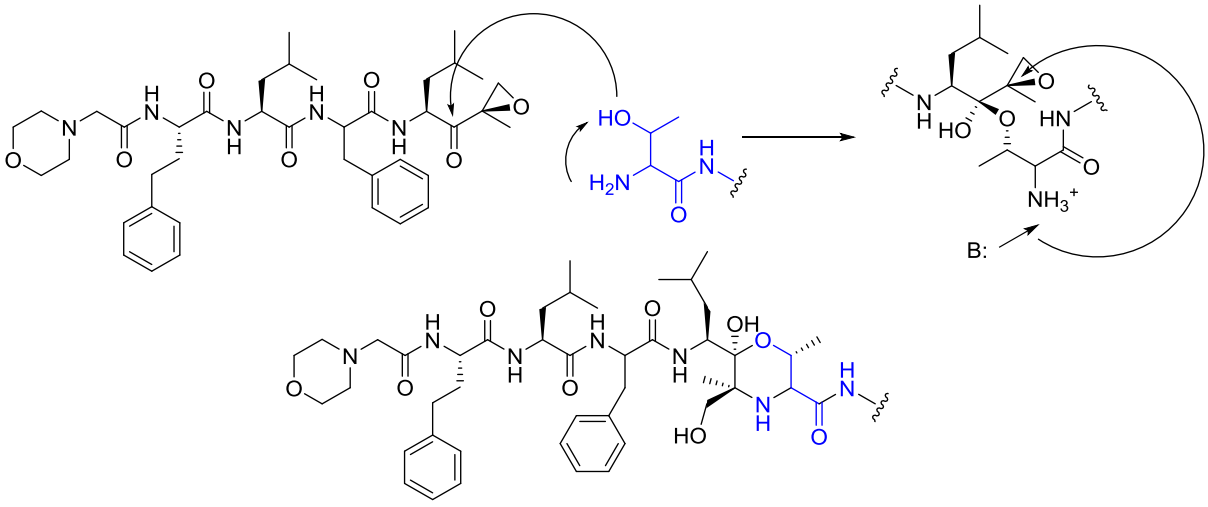

Epoxyketone Inhibitor Mechanism (Carfilzomib)

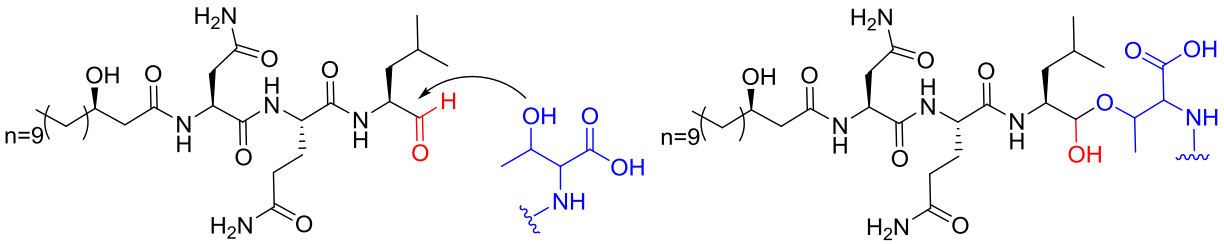

Peptidyl Aldehyde Inhibitor Mechanism (fellutamide B)

The schemes shown above all demonstrate the mechanism of action for the corresponding drugs. The common theme for every drug is the formation of a covalent bond between the secondary hydroxy of the Threonine residue with an electrophilic group whether it is a carbonyl or a boronic acid moiety. The boronic acid and peptidyl aldehyde inhibitors form a reversible covalent linkage through formation of a hemiacetal-like intermediate which can be hydrolyzed back to the corresponding free acid and 2° hydroxyl of the Threonine. Both the β-lactone and epoxyketone inhibitors form irreversible covalent linkages with the Threonine residue within the 20S proteasome. In the case of the salinosporamide A the Threonine residue gets deprotonated which then opens the lactone through nucleophilic attack of the carbonyl. The resulting free alcohol then becomes deprotonated and subsequently displaces the primary chlorine through an SN2 reaction to create a tetrahydrofuran. This furan can then H-bond to the primary amine of the Threonine residue creating a very stable intermediate that is irreversibly bound. In the case of the

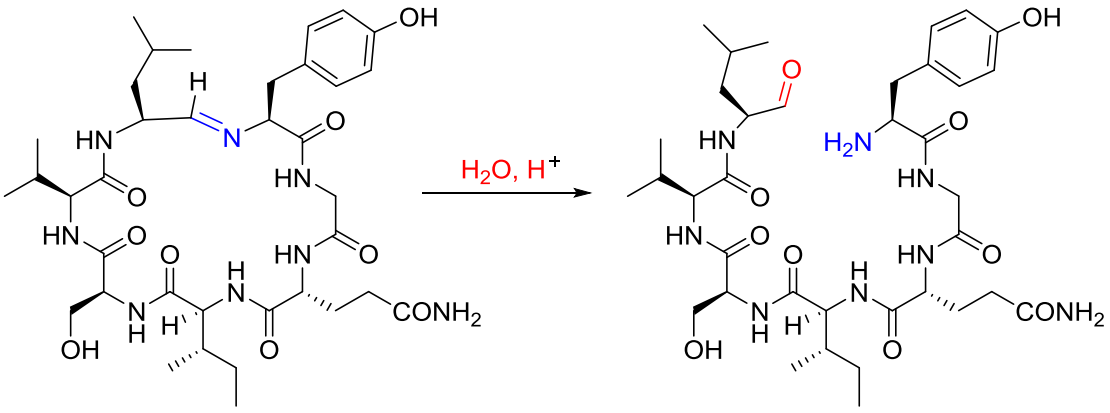

Figure 22 Proposed hydrolysis of the imine to the corresponding peptidyl aldehyde

epoxyketone inhibitor the deprotonated Threonine hydroxyl attacks the α-ketone to the Leucine residue. The primary amine then becomes deprotonated which then allows epoxide opening with the nucleophilic amine to occur to form a morpholine ring. Since Scytonemide A contains the unique imine linkage we propose that its mechanism of action is most similar to peptidyl aldehyde inhibitor fellutamide B. One possible mechanism for its proteasome activity involves the hydrolysis of the imine to the corresponding peptidyl aldehyde and the free amine, seen in **figure 22**, which can then go through the same type of mechanism reported for fellutamide B. An alternative proposed mechanism is the direct addition of the Threonine residue in the chymotrypsin subunit to the protonated imine. The imine would be predicted to have similar reactivity to an aldehyde which leads us to believe you could get direct formation of the hemiaminal seen in **figure 23**. It is important to note that both of these mechanisms would proceed through a reversible process.

In order to elucidate the actual mechanism of action as well as perform more biological studies it is paramount that more scytonemide A is synthesized. The isolation process was only able to isolate 1.2 mg of pure scytonemide A from 8 liters of cell culture[20]. In order to obtain more scytonemide A, a synthetic scheme had to be developed that would allow quick and facile production of the natural product as well as allow quick and easy modification to create structural analogues and mechanistic probes.

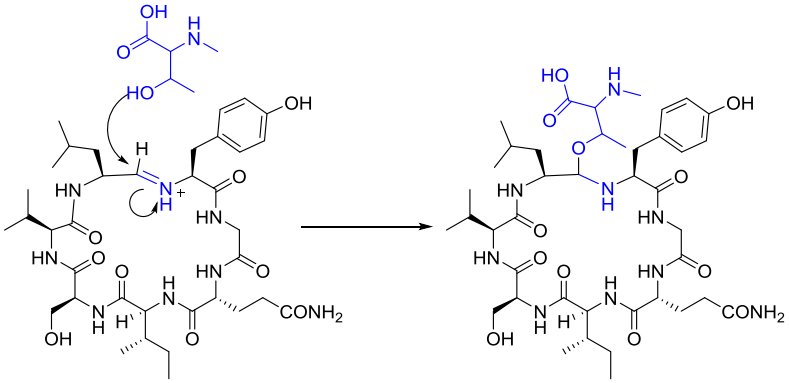

Figure 23 Hemiaminal formation resulting in reversible inhibition of the 20S

The Total Synthesis of Scytonemide A

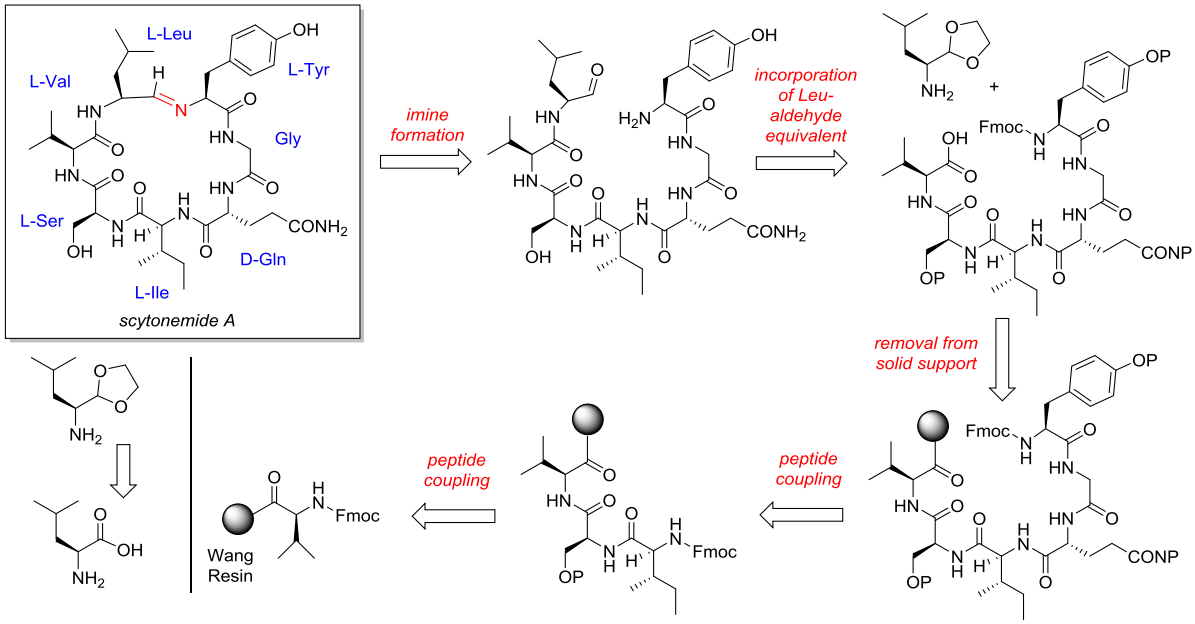

Scheme 2 The retrosynthesis of scytonemide A

In order to synthesize scytonemide A we first had to perform a retrosynthesis, seen in **scheme 2** above, that we could employ for the forward synthesis of this novel secondary metabolite. We envisioned that the imine linkage could be formed from a C terminal peptidyl aldehyde on a Leucine residue with an N terminal primary amine on the tyrosine residue. Mahariel *et al.* has reported the *in situ* macrocylization of nostocyclopeptide through the formation of an imine linkage of a peptidyl aldehyde at the C terminus with a primary amine at the N terminus[22]. The synthesis of the polypeptide would be done *in situ* via a solid phase protein synthesis (SPPS) of fluorenylmethyloxycarbonyl (Fmoc) protected amino acids. The first residue that would be used in the SPPS would be a valine residue that is covalently bound to a polystyrene Wang resin at the C terminus leaving an Fmoc protected N terminus. Subsequent deprotection of the Fmoc under basic conditions would afford a primary amine that could undergo subsequent coupling with the next Fmoc protected amino acid in sequence. The Wang resin is acid labile which means that we wanted to employ acid labile protecting groups on the

chemically reactive side chains of the Serine, Glutamine, and Tyrosine residues. Once the six residue polypeptide is created, the side chains of the molecule could be globally deprotected and the valine residue cleaved from the solid support. In order to create the necessary peptidyl aldehyde derivative of Leucine, seen in the bottom left of **scheme 2**, the amino acid would be synthetically modified prior to coupling with the polypeptide. In order to achieve this, the aldehyde of the Leucine would be protected as an acetal in order to prevent polymerization of the peptidyl aldehyde and the free amine of the final product after deprotection of the Cbz protecting group on the amine. Oxidation of the primary alcohol to the aldehyde was envisioned to be accomplished via a Swern oxidation of L-Leucinol which would be derived from an LAH reduction of Leucine followed by a Cbz protection of the primary amine.

The Forward Synthesis of the Leu/Ala Peptidyl Aldehyde

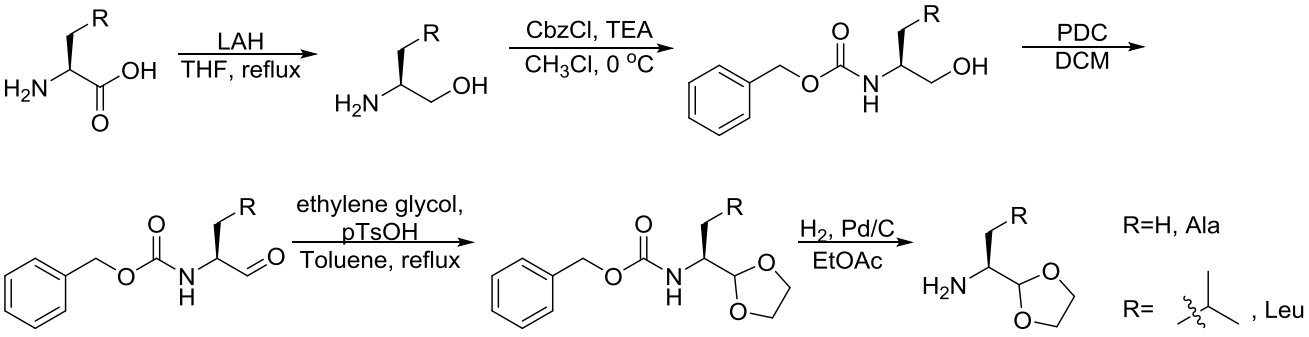

Scheme 3 The optimized forward synthesis of the modified leu/ala residue

The forward synthesis starts with pure L-Leucine which undergoes an LAH reduction to generate the primary alcohol. The reaction went to completion according to TLC and purification of the crude product was difficult due to the high polarity of the product. Initially it appeared that the Cbz protection of the free amine was unsuccessful, although it was later determined that the product of the LAH reduction was very unstable and the crude material had to be carried forward immediately after workup. The resulting carbamate product was stable and easily purified via

flash column chromatography. According to the synthetic plan, this material was subjected to Swern oxidation conditions to affect the oxidation of the primary alcohol to the corresponding aldehyde. Multiple attempts were made to carry out this conversion, however, they only afforded starting material. Based on these results we decided to switch to stronger oxidizing agents such as Dess-Martin Periodane and IBX, although neither of these oxidants proved to be successful either. Successful oxidation to the aldehyde was finally achieved upon treatment of the primary alcohol with PDC. The acetal protected aldehyde was then generated after being treated with ethylene glycol and catalytic p-toluenesulfonic acid in toluene. A Dean-Stark apparatus was used to remove the water formed during formation of the acetal and to drive the reaction to completion. Removal of the Cbz protecting group is to be done with H_2, Pd/C in EtOAc to afford the final product, but this has not been carried out to date.

This same synthetic scheme has been used on L-Alanine to facilitate the Alanine scan that we envision performing. Alanine and Leucine both contain a lipophilic side chain that is chemically inert which is why we were able to utilize the same scheme on a different amino acid.

The Solid Phase Protein Synthesis of Scytonemide A

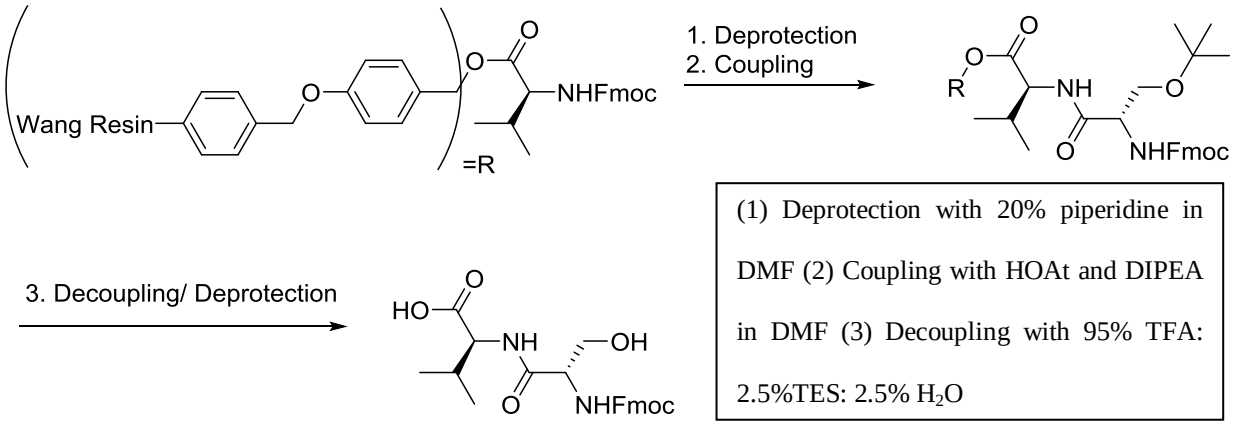

Scheme 4 Optimized conditions for the SPPS

SPPS will be utilized to construct the first six residues of scytonemide A. This has not yet been accomplished. We have optimized the conditions, however, that are going to be used in order to generate the polypeptide. The resin beads containing the valine residue could be sufficiently swelled in DMF for 3 hours prior to coupling. After rinsing the beads three times with DMF, a 20% solution of piperidine in DMF was added and the mixture was allowed to stir on an orbital shaker for 2.5 hours. This solution was washed from the beads by 3 additions of DMF and then then the coupling reagents, HOAt and DIPEA in DMF, were added to the beads. This mixture remained on the orbital shaker for 3 hours before being washed three times with DMF. After washing and filtering of the beads, a solution of 95% TFA: 2.5% TES: and 2.5% H_2O was added which acted as the decoupling and deprotection solution. This mixture was allowed to stir for 2.5 hours and then the product was removed from the beads by filtration through a Buchner funnel. The solution was then pumped down via vacuum filtration and the organics were extracted with diethyl ether. The decoupled product seen in **scheme 4** was soluble in the organic layer. Although this was somewhat surprising, the Fmoc group is likely

responsible for making the molecule lipophilic enough to be extracted into the organic layer as opposed to the aqueous layer. After the final Fmoc deprotection (prior to decoupling and deprotection) the polypeptide will most likely stay in the aqueous layer and all of the organics will be extracted into the organic layer.

Future Works

The most important goal that we have yet to achieve is the total synthesis of scytonemide A. Once the linear polypeptide is created and cleaved from the Wang resin, we want to attach the peptidyl aldehyde residue to the C terminus of the valine. After this step we merely have to deprotect the Fmoc group on the N terminus tyrosine and the acetal on the C terminus.

Once the total synthesis has been completed we want to utilize the procedures that we have already created to perform an Alanine scan on all of the amino acids, including the peptidyl aldehyde of Leucine, contained in scytonemide A. This will help us probe the biological significance of each amino acid in the protein because Alanine is a chemically inert, non-bulky, methyl functional group that contains the same stereochemistry as most of the AA's.

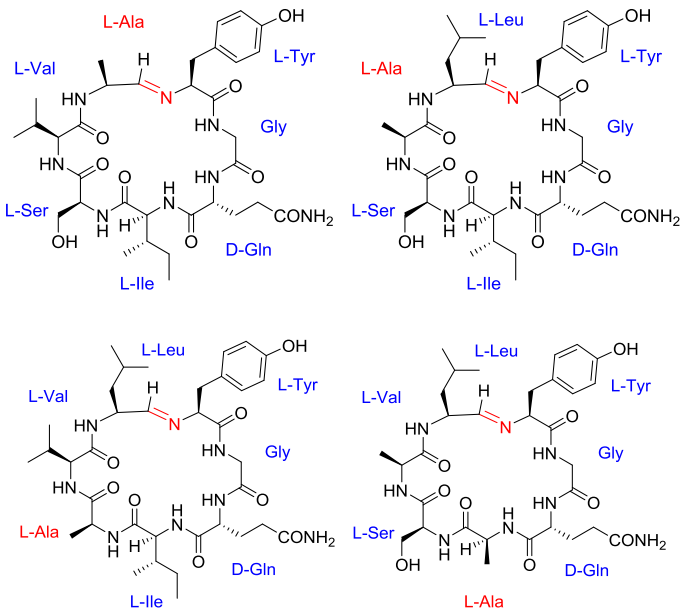

Figure 24 The Alanine Scan of Scytonemide A

The last goal for our future work on this project is to determine the mechanism of action of scytonemide A through structural modification of the natural product. In order to determine if the linear peptidyl aldehyde is responsible for the inhibition we want to prevent the cyclization of scytonemide A. In order to do this we have to methylate the N terminal amine prior attachment of the peptidyl aldehyde residue which will prevent imine formation upon coupling and deprotection of the acetal.

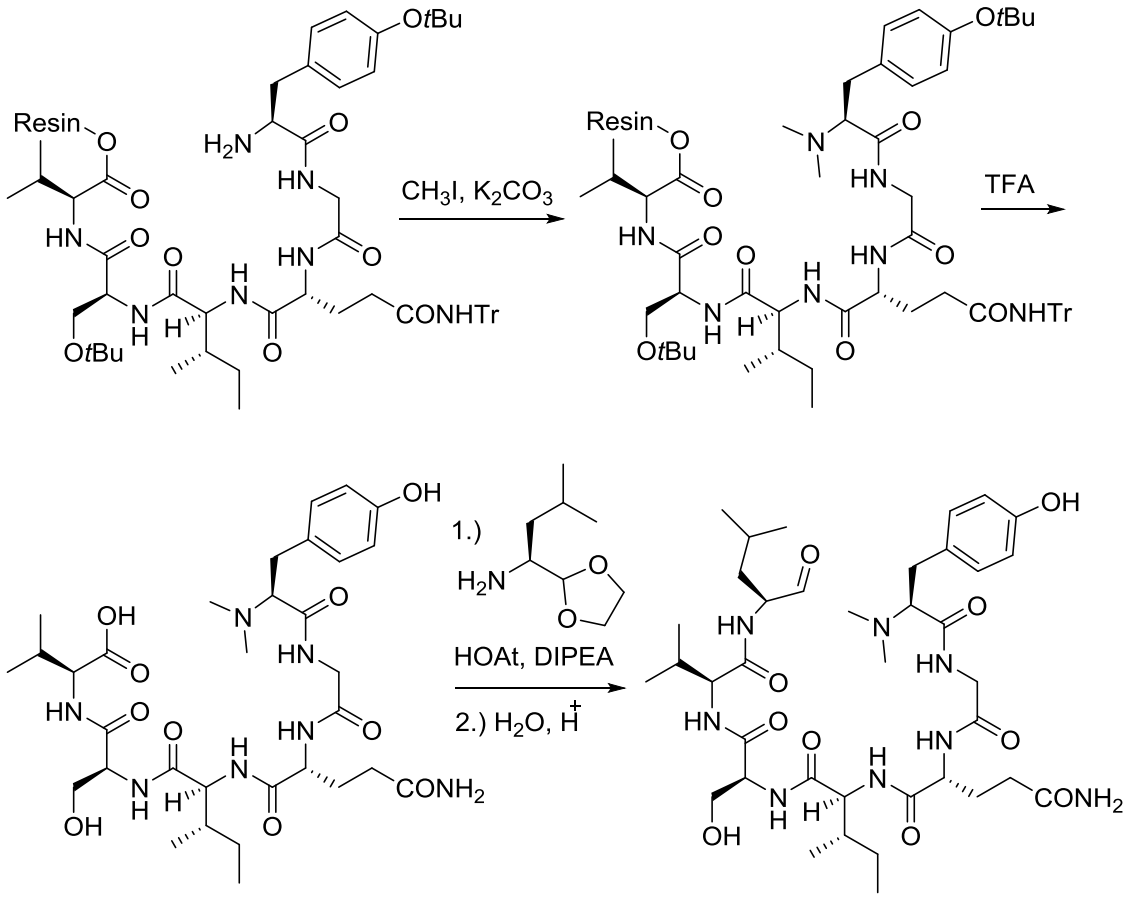

Scheme 5 The Linear derivative of scytonemide A

Part III: Experimentals

TBS protection of the C3 alcohol pregnenolone

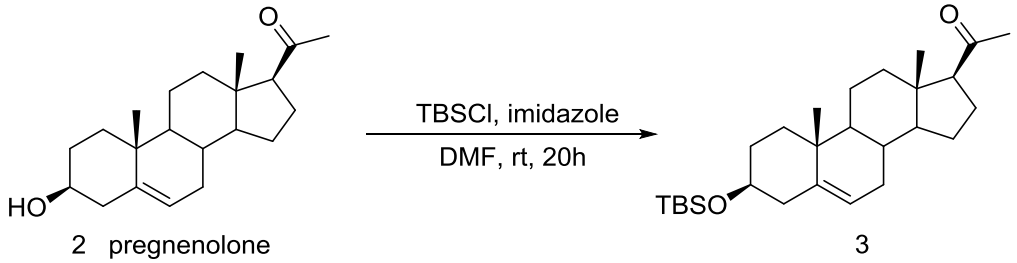

2 pregnenolone 3

A solution of Pregnenolone, **2**, (3.000 g, 9.749 mmol), tert-butyldimethylsilyl chloride (2.143 g, 14.21 mmol), and imidazole (0.807 g, 11.85 mmol) in DMF (158 mL) was reacted at 21 °C overnight. The reaction mixture was quenched with cold deionized water. The resulting white precipitation, **3**, was collected via vacuum filtration and washed with cold deionized water (3X10 mL) to obtain pure silylated product (3.896 g, 9.045 mmol, 95%) as a white powder: mp 163 °C; 1H NMR (CDCl3, 400 MHz) δ 5.31 (m, 1H), 3.48 (m, 1H), 2.53 (t, 1H), 2.12 (s, 3H), 0.99 (s, 3H), 0.88 (s, 9H), 0.62 (s, 3H), 0.05 (s, 6H); 13C NMR (CDCl3, 100 MHz) δ 209.5, 141.5, 120.8, 72.5, 63.7, 56.9, 50.0, 43.9, 42.7, 38.8, 37.3, 36.5, 32.0, 31.8, 31.7, 31.5, 25.9, 24.4, 22.7, 21.0, 19.4, 18.2, 13.2, -4.6; IR (film): 1701 cm−1; HRMS-TOF m/z (M + Na)+ calcd for C27H46O2Si 453.3165, found 453.3165.

General procedure for the alkylation:

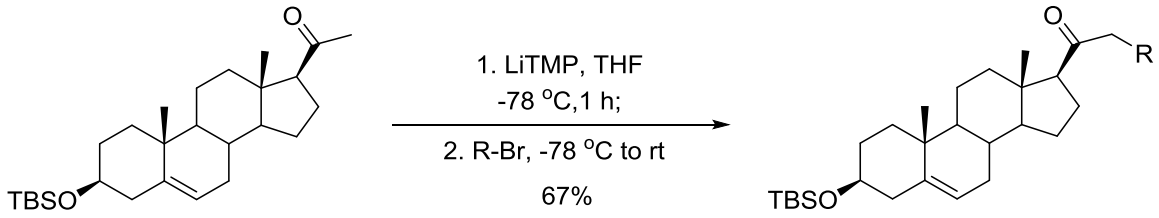

To a solution of tetramethylpiperidine (0.357 mL, 2.114 mmol) in THF (14.1 mL) at -78 °C was added n-butyl lithium (2.5 M in hexanes, 0.790 mL, 1.973 mmol). The resulting solution was

allowed to stir for 35 minutes at -78 °C before the addition of a solution of 3 (0.6072 g, 1.410 mmol) in THF (5.7 µL). After 3 h of stirring at -78 °C, the alkylating agent (0.1755 mL, 2.819 mmol) was added drop wise to the reaction mixture, warmed to 21 °C, and stirred overnight. The reaction was quenched with excess aqueous ammonium chloride. The separated and aqueous layer was extracted with ethyl acetate. The combined organic layers were then dried with anhydrous sodium sulfate and concentrated under reduced pressure. The crude product was purified by silica gel column chromatography (EtOAc:DCM:hexanes, 1:1:98) to afford pure mono-alkylated product as a white solid.

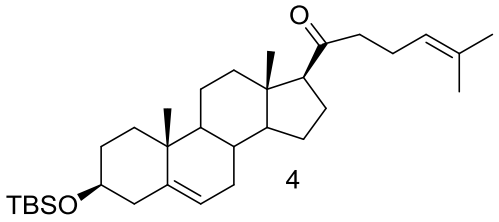

Monoalkylated sterol. (0.397 g, 68%) The general alkylation procedure was utilized with dimethylallyl bromide as the alkylating reagent to generate compound **4** as a white solid mp 120-121 °C; 1H NMR (CDCl3, 400 MHz) δ 5.31 (d, 1H), 5.06 (t, 1H), 3.48 (m, 1H), 2.50 (t, 1H), 2.39 (m, 2H), 2.21 (m, 5H), 2.00 (m, 2H), 1.81 (m, 1H), 1.66 (s, 3H), 1.61 (s, 3H), 1.48 (m, 3H), 0.99 (s, 3H), 0.88 (s, 9H), 0.60 (s, 3H), 0.05 (s, 6H); 13C NMR (CDCl3, 100 MHz) δ 211.6, 141.9, 132.8, 123.6, 121.3, 72.9, 63.3, 57.4, 50.5, 44.7, 44.6, 43.2, 39.4, 37.8, 37.0, 32.5, 32.3, 32.2, 26.3, 26.1, 24.9, 23.3, 22.8, 21.5, 19.8, 18.6, 18.0, 13.8, -4.1; IR (film): 1704 cm−1; HRMS-TOF m/z (M + Na)+ calcd for C32H54O2Si 521.3791, found 521.3814.

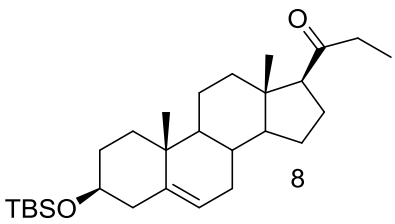

Monoalkylated sterol. (0.380 g, 60%) The general alkylation procedure was utilized with iodomethane as the alkylating reagent to generate compound **8** as a white solid: ^{1}H NMR (400 MHz, $CDCl_3$) δ 5.72 (s, 1H), 4.87 (d, *J* = 1.3 Hz, 1H), 4.77 (s, 1H), 1.17 (s, 3H), 1.01 (t, *J* = 7.4 Hz, 3H), 0.60 (s, 3H); ^{13}C NMR (101 MHz, $CDCl_3$) δ 199.53, 171.47, 150.87, 123.80, 108.48, 56.12, 55.78, 53.97, 43.08, 38.64, 38.51, 36.03, 35.72, 33.98, 32.91, 31.97, 30.29, 25.81, 24.11, 21.10, 17.40, 12.83.

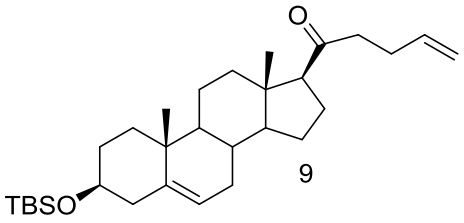

9

Monoalkylated sterol. (0.256 g, 44%) The general alkylation procedure was utilized with allyl bromide as the alkylating reagent to generate compound **9** as a white solid: mp: ^{1}H NMR (300 MHz, $CDCl_3$) δ 5.82 (ddt, *J* = 16.6, 10.2, 6.4 Hz, 2H), 5.33 (d, *J* = 5.0 Hz, 2H), 5.09 – 4.94 (m, 4H), 3.56 – 3.44 (m, 2H), 2.47 (d, *J* = 7.1 Hz, 3H), 1.01 (s, 6H), 0.90 (s, 17H), 0.63 (s, 5H), 0.08 (d, *J* = 4.0 Hz, 12H); ^{13}C NMR (101 MHz, $CDCl_3$) δ 211.03, 141.93, 137.95, 121.28, 115.48, 72.94, 63.38, 57.41, 50.47, 44.65, 43.82, 43.17, 39.36, 37.78, 37.00, 32.44, 32.26, 32.23, 30.12, 28.17, 26.34, 24.94, 23.34, 21.47, 19.83, 18.67, 13.80, -4.18.

General procedure for the wittig olefination:

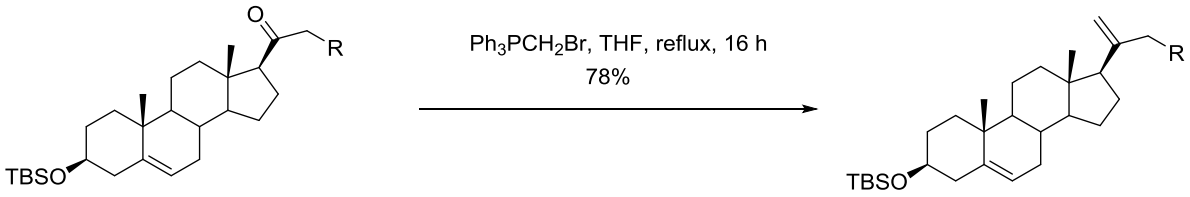

To a solution of methyltriphenylphosphonium bromide (3.940 g, 11.02 mmol) in THF (5.5 mL) at 0 °C was added n-butyl lithium (2.5 M in hexanes, 4.19 mL, 10.47 mmol). The resulting

reaction mixture was stirred at 0 °C for 1 hour before adding a solution of the alkylated product (0.550 g, 1.102 mmol) in THF (5.5 mL). The reaction was brought to reflux and stirred overnight before being quenched with deionized water. The organic layer was removed and the aqueous layer was extracted three times with ethyl acetate. Combined organic layers were dried over anhydrous sodium sulfate and concentrated under reduced pressure. Crude product was then purified via silica gel column chromatography (DCM:EtOAc:hexanes, 1:1:98) to obtain the olefinated compound as a pure solid.

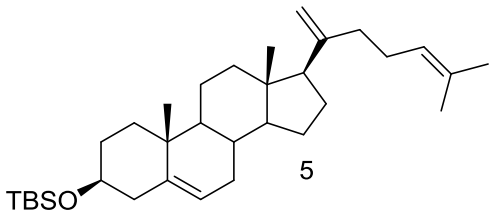

Olefinated product. (0.489 g, 0.984 mmol, 89%) The general olefination procedure utilized compound **4** to generate compound **5** as a white solid as a white solid: mp 86 °C; 1H NMR (CDCl3, 400 MHz) δ 5.31 (d, J = 5.1 Hz, 1H), 5.10 (m, 1H), 4.87 (s, 1H), 4.78 (s, 1H), 3.48 (m, 1H), 2.26 (m, 1H), 2.07 (m, 7H), 1.79 (m, 3H), 1.68 (s, 3H), 1.61 (s, 3H), 1.51 (s, 10H), 1.18 (m, 3H), 0.99 (s, 3H), 0.88 (s, 9H), 0.57 (s, 3H), 0.05 (s, 6H); 13C NMR (CDCl3, 400 MHz) δ 149.3, 141.5, 131.4, 124.3, 121.0, 72.5, 71.8, 56.6, 55.9, 50.3, 43.0, 42.7, 38.7, 37.3, 36.6, 32.2, 31.8, 27.1, 25.9, 25.8, 25.7, 21.1, 19.4, 18.2, 17.7, 12.7, 13.3, -4.5; IR (film): 2928 cm−1.

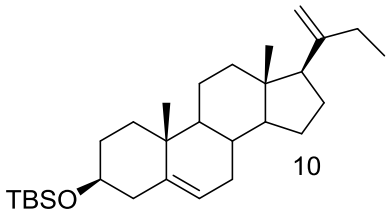

Olefinated product (0.3162 g, 86%) The general olefination procedure utilized compound **8** to generate compound **10** as a white solid as a white solid: ^{1}H NMR (300 MHz, $CDCl_3$) δ 5.33 (d, *J*

= 4.6 Hz, 1H), 4.87 (s, 1H), 4.78 (s, 1H), 3.56 – 3.43 (m, 1H), 1.04 (d, *J* = 7.4 Hz, 3H), 1.01 (s, 4H), 0.90 (s, 10H), 0.58 (s, 3H), 0.07 (s, 6H).

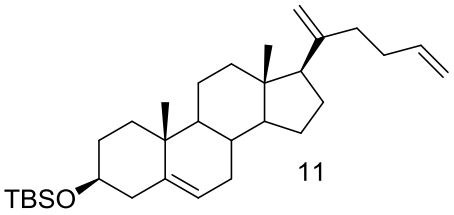

11

Olefinated product (0.0417 g, 43%) The general olefination procedure utilized compound **9** to generate compound **11** as a white solid as a white solid: ^{1}H NMR (300 MHz, $CDCl_3$) δ 5.91 – 5.75 (m, 1H), 5.32 (d, *J* = 5.2 Hz, 1H), 5.07 – 4.91 (m, 2H), 4.88 (s, 1H), 4.81 (s, 1H), 3.57 – 3.34 (m, 1H), 1.01 (s, 3H), 0.91 – 0.88 (m, 9H), 0.59 (s, 3H), 0.08 – 0.05 (m, 6H); ^{13}C NMR (101 MHz, $CDCl_3$) δ 149.16, 141.19, 139.14, 122.02, 114.78, 110.09, 72.17, 57.06, 56.38, 50.66, 43.50, 42.69, 39.09, 37.66, 37.39, 36.96, 33.10, 32.69, 32.22, 32.04, 30.12, 26.24, 24.61, 21.54, 19.84, 13.17.

General procedure for the TBAF deprotection:

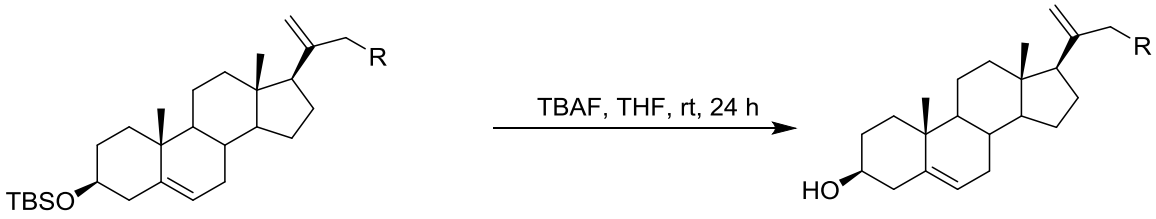

A solution of A (0.124 g, 0.250 mmol) and tetrabutylammonium fluoride (1.0 M in THF, 0.5 mL, 0.5 mmol) in THF (1.25 mL) was stirred at 21 °C overnight. The reaction mixture was concentrated under reduced pressure and the resulting residue was purified by silica gel column chromatography (EtOAc-hexanes, 3:17) to give the deprotected product.

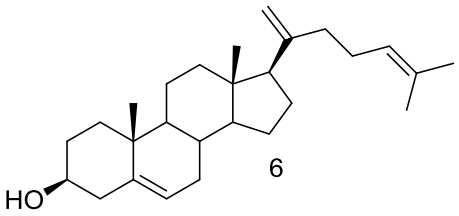

Deprotected product (0.094 g, 94%) The general TBAF deprotection procedure was utilized with compound **5** as the starting material to produce compound **6** as a white solid: mp 89-91 °C; 1H NMR (CDCl3, 400 MHz) δ 5.35 (d, J = 5.0 Hz, 1H), 5.11 (m, 1H), 4.87 (s, 1H), 4.78 (s, 1H), 3.52 (m, 1H), 2.27 (m, 2H), 2.05 (m, 6H), 1.82 (m, 4H), 1.68 (s, 3H), 1.60 (s, 3H), 1.49 (s, 7H), 1.11 (m, 6H), 1.00 (s, 3H), 0.57 (s, 3H); 13C NMR (CDCl3, 400 MHz) δ 149.2, 140.7, 131.4, 124.3, 121.6, 109.3, 71.8, 71.7, 56.6, 55.9, 50.2, 43.0, 42.2, 38.6, 37.6, 37.2, 36.5, 32.2, 31.8, 31.6, 27.1, 25.8, 25.7, 24.2, 21.1, 19.4, 17.7, 12.7; HRMS-TOF m/z (M + Na)+ calcd for C27H42O 405.3133, found 405.3151.

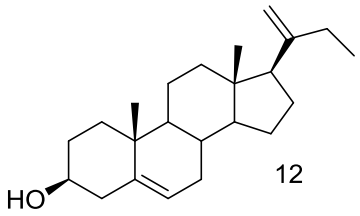

Deprotected product (0.217 g, 93%) The general TBAF deprotection procedure utilized compound **10** to produce compound **12** as a white solid: ^{1}H NMR (300 MHz, $CDCl_3$) δ 5.36 (d, *J* = 5.2 Hz, 1H), 4.86 (s, 1H), 4.77 (s, 1H), 3.53 (ddd, *J* = 15.4, 10.9, 4.5 Hz, 1H), 1.02 (dd, *J* = 9.2, 5.5 Hz, 7H), 0.57 (s, 3H).

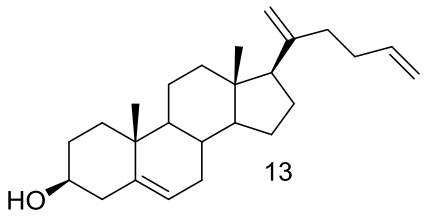

Deprotected product (0.0207g, 66%) The general TBAF deprotection procedure utilized compound **11** to produce compound **13** as a white solid: ^{1}H NMR (300 MHz, $CDCl_3$) δ 5.81 (ddt, *J* = 16.7, 10.1, 6.4 Hz, 2H), 5.34 (d, *J* = 5.3 Hz, 2H), 5.08 – 4.92 (m, 4H), 3.52 (ddd, *J* = 15.5, 11.0, 4.5 Hz, 2H), 1.25 (s, 5H), 1.00 (s, 6H), 0.62 (s, 5H).

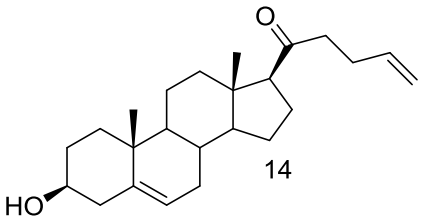

14

Deprotected product (0.218g, 50%) The general TBAF deprotection procedure utilized compound **9** to produce compound **14** as a white solid: ^{1}H NMR (300 MHz, $CDCl_3$) δ 5.90 – 5.70 (m, 2H), 5.34 (d, *J* = 5.3 Hz, 2H), 5.10 – 4.91 (m, 4H), 3.52 (ddd, *J* = 15.5, 11.0, 4.5 Hz, 2H), 1.24 (d, *J* = 6.4 Hz, 5H), 1.00 (s, 6H), 0.62 (s, 5H).

General procedure for the oppenaeur oxidation

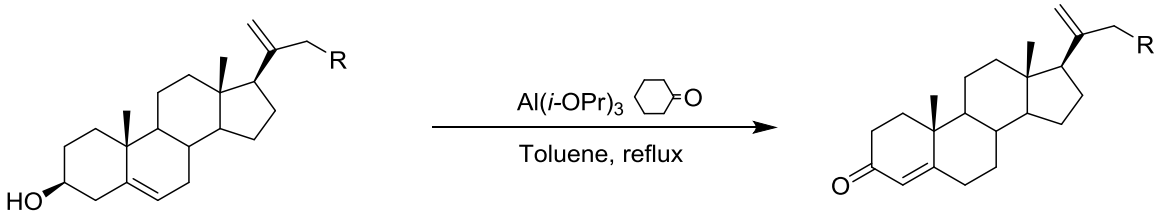

To a solution of A (0.434 g, 1.135 mmol) and cyclohexanone (1.175 mL, 11.35 mmol) in toluene (22.7 mL) at reflux was added aluminum isopropoxide (0.116 g, 0.568 mmol). The reaction was stirred at reflux overnight. The reaction mixture was concentrated under reduced pressure, taken up in deionized water, and extracted three times with ethyl acetate. Crude product was purified by silica gel column chromatography (EtOAc:hexanes, 1:19) to afford the completed analogue.

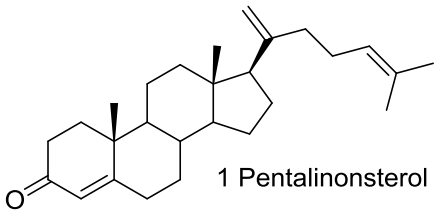

1 Pentalinonsterol

Oppenaeur product (0.386 g, 89%) The general oppenaeur procedure was utilized to afford **1** (pentalinonsterol) as a white solid: mp 89-91 °C; 1H NMR (CDCl3, 400 MHz) δ 5.35 (d, J = 5.0 Hz, 1H), 5.11 (m, 1H), 4.87 (s, 1H), 4.78 (s, 1H), 3.52 (m, 1H), 2.27 (m, 2H), 2.05 (m, 6H), 1.82 (m, 4H), 1.68 (s, 3H), 1.60 (s, 3H), 1.49 (s, 7H), 1.11 (m, 6H), 1.00 (s, 3H), 0.57 (s, 3H); 13C NMR (CDCl3, 400 MHz) δ 149.2, 140.7, 131.4, 124.3, 121.6, 109.3, 71.8, 71.7, 56.6, 55.9, 50.2, 43.0, 42.2, 38.6, 37.6, 37.2, 36.5, 32.2, 31.8, 31.6, 27.1, 25.8, 25.7, 24.2, 21.1, 19.4, 17.7, 12.7; HRMS-TOF m/z (M + Na)+ calcd for C27H42O 405.3133, found 405.3151.

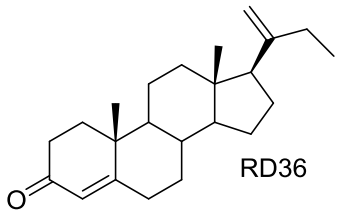

RD36

Oppenaeur product (0.150 g, 69%) The general oppenaeur procedure was utilized to afford **x** as a white solid:

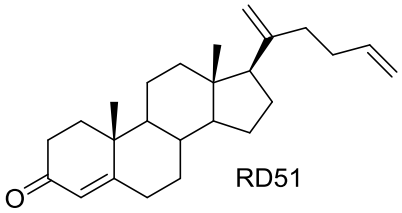

RD51

Oppenaeur product (6.89 mg, 33%) The general oppenaeur procedure was utilized to afford **x** as a white solid: ^{1}H NMR (300 MHz, $CDCl_3$) δ 5.88 – 5.75 (m, 1H), 5.73 (s, 1H), 5.07 – 4.93 (m, 2H), 1.18 (s, 3H), 0.66 (s, 3H).

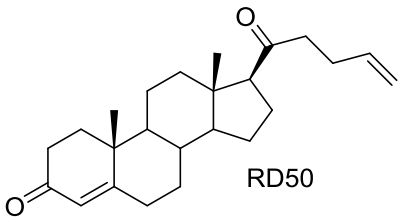

RD50

Oppenaeur product (4.12 mg, 19%) The general oppenaeur procedure was utilized to afford **x** as a white solid: ^{1}H NMR (300 MHz, $CDCl_3$) δ 5.81 (ddd, *J* = 16.6, 10.3, 6.2 Hz, 1H), 5.73 (s, 1H), 4.98 (dd, *J* = 19.3, 13.9 Hz, 2H), 4.90 (s, 1H), 4.81 (s, 1H), 1.18 (s, 3H), 0.62 (s, 3H).

General procedure for the LAH reduction

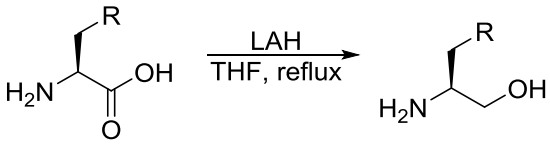

To a 0 °C solution of THF (9.5 mL) was added LAH portion wise (0.3727 g, 9.822 mmol) followed by the addition of the L-amino acid (0.250 g, 2.806 mmol). This reaction was refluxed overnight and then quenched via the Fieser method. The product was extracted three times with EtOAc, and concentrated *in vacuo*. The crude oil was checked by ^{1}H NMR and then immediately carried forward into the next reaction without further purification.

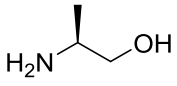

15

Reduced product (crude 0.320 g) The general procedure for the LAH reduction was utilized to afford the product, **15**, as a yellow oil from the starting material, L-Alanine. ^{1}H NMR (300 MHz, $CDCl_3$) δ 3.54 (ddd, *J* = 10.5, 4.0, 0.4 Hz, 1H), 3.23 (dd, *J* = 10.5, 7.8 Hz, 1H), 3.01 (dqd, *J* = 12.9, 6.4, 4.0 Hz, 1H), 1.05 (dd, *J* = 6.4, 0.5 Hz, 3H).

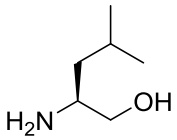

20

Reduced product (crude 0.4817 g) The general procedure for the LAH reduction was utilized to afford the product, **20,** as a yellow oil from the starting material, L-Leucine. ^{1}H NMR (400 MHz, $CDCl_3$) δ 3.42 – 3.34 (m, 1H), 3.07 (dd, *J* = 10.5, 8.1 Hz, 1H), 2.74 (dt, *J* = 14.5, 5.3 Hz, 1H), 1.61 – 1.45 (m, 1H), 1.02 (t, *J* = 7.0 Hz, 2H), 0.75 (dd, *J* = 10.9, 6.6 Hz, 6H).

General procedure for the Cbz protection

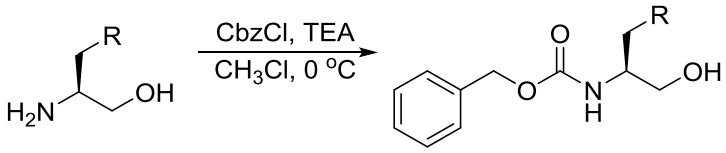

Benzyl chloroformate (0.821 mL, 5.753 mmol) was added slowly to a precooled (0 °C) solution of the reduced amino acid (0.482 g, 4.110 mmol) and triethylamine (0.858 mL, 6.165 mmol) in chloroform (20.5 mL). The reaction was allowed to stir overnight and warm to room temperature before it was evaporated under reduced pressure. Ethyl acetate was added to the resulting oil and then the solution was washed with 1M NaOH, brine, and dried with $MgSO_4$. The resulting residue was purified via flash column chromatography (EtOAc: Hexanes, 2:3)

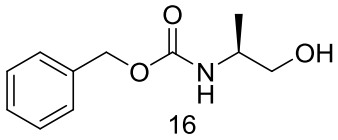

16

Cbz protected product (0.6439 g, 3.077 mmol) The general Cbz protection procedure utilized compound **15** to afford the product, **16**, as a white sold. ^{1}H NMR (300 MHz, $CDCl_3$) δ 7.37 – 7.29 (m, 6H), 5.09 (s, 2H), 3.89 – 3.77 (m, 1H), 3.64 (dd, *J* = 11.0, 3.9 Hz, 1H), 3.51 (dd, *J* =

11.0, 5.9 Hz, 1H), 1.16 (d, *J* = 6.8 Hz, 3H); ^{13}C NMR (101 MHz, $CDCl_3$) δ 156.68, 136.42, 128.59, 128.21, 128.17, 66.85, 66.60, 48.97, 17.28.

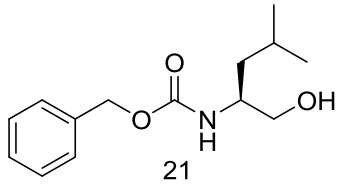

21

Cbz protected product (0.356 g, 1.416 mmol) The general Cbz protection procedure utilized compound **20** to afford the product, **21**, as a white sold. ^{1}H NMR (400 MHz, $CDCl_3$) δ 7.37 – 7.27 (m, 10H), 5.08 (s, 4H), 3.78 (d, *J* = 3.4 Hz, 2H), 3.65 (d, *J* = 10.2 Hz, 2H), 3.51 (s, 2H), 1.70 – 1.58 (m, 2H), 1.38 – 1.25 (m, 4H), 0.92 (d, *J* = 6.4 Hz, 11H).

General procedure for PDC oxidation

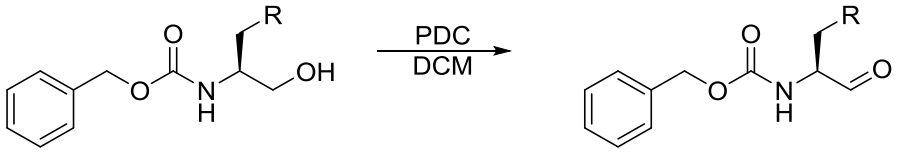

To a solution of Cbz protected amino acid (80.6 mg, 0.3852 mmol) in DCM and cooled to 0 °C was added pyridinium dichromate (0.432 g, 2.003 mmol) and allowed to stir overnight. The solution was filtered through celite and concentrated *in vacuo*. The residue was purified via flash column chromatography (EtOAc: Hexanes, 27:83)

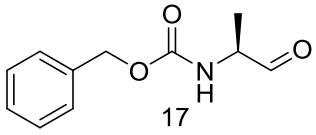

17

PDC oxidation product (78.9 mg, 0.381 mmol) The general PDC oxidation procedure used compound **16** as the starting material to afford compound **17** a white solid. ^{1}H NMR (300 MHz, $CDCl_3$) δ 9.54 (s, 4H), 7.36 (s, 26H), 5.12 (s, 9H), 4.37 – 4.20 (m, 4H), 2.42 (s, 2H), 1.36 (d, *J* = 7.3 Hz, 14H).

Acetal Formation for the Alanine derivative

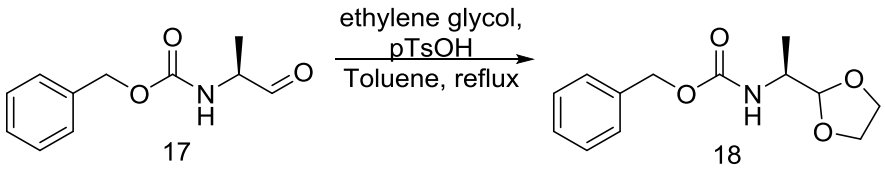

The Cbz protected Alaninal was dissolved in toluene (6.35 mL) to which ethylene glycol (0.320 mL, 5.711 mmol) and p-toluenesulfonic acid (0.029 g, 0.152 mmol) were added. The mixture was refluxed overnight, concentrated under reduced pressure, and subsequently taken up in DCM. The mixture was washed 3 times with H_2O and $NaHCO_3$ and concentrated under reduced pressure. The presence of the desired product, **18**, was confirmed by ^1H NMR

SPPS: Deprotection of the Fmoc and amino acid coupling procedure

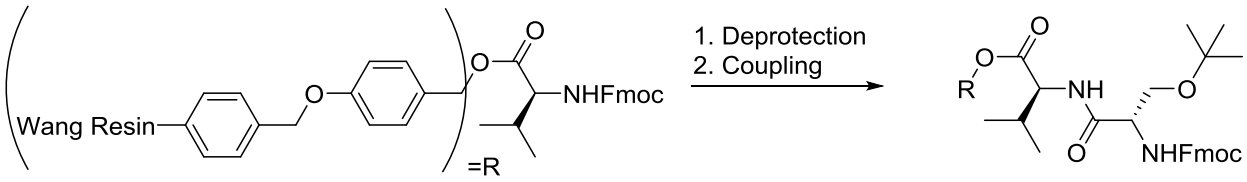

After the Wang resin is swelled in DMF for 3 hours and washed three times with DMF a solution of 20% piperidine in DMF is added and allowed to shake at 21°C for 30 minutes. The solution is then filtered and washed with DMF 3 times upon which 2 equivalents (based on resin substitution) of the protected amino acid dissolved in DMF (5 mL/ gram of resin) is added. HATU (2 equivalents) is subsequently added with DIPEA (4 equivalents) and the mixture is allowed to stir for 2.5 hours before the deprotection sequence may be run again.

SPPS: Global side chain deprotection and Wang resin decoupling

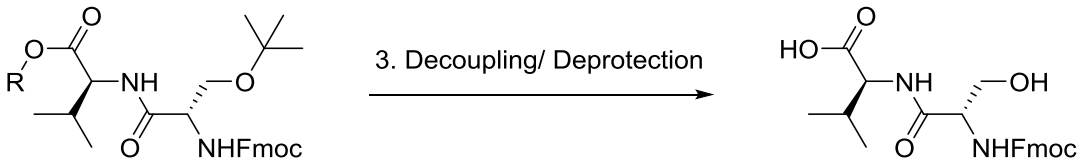

The resin-bound polypeptide is placed in a solution (4 times the height of the swelled beads) of 95:2.5:2.5 TFA:TES:H_2O and stirred for three hours. The decoupled and deprotected product was removed by vacuum filtration and the product was extracted with 0 °C diethyl ether.

References

(1) WHO | Leishmaniasis http://www.who.int/mediacentre/factsheets/fs375/en/ (accessed Mar 26, 2015).

(2) WHO | The vector http://www.who.int/leishmaniasis/vector/en/ (accessed Mar 26, 2015).

(3) Prevention, C.-C. for D. C. and. CDC - Leishmaniasis - Biology http://www.cdc.gov/parasites/leishmaniasis/biology.html (accessed Mar 26, 2015).

(4) Prevention, C.-C. for D. C. and. CDC - Leishmaniasis - Resources for Health Professionals http://www.cdc.gov/parasites/leishmaniasis/health_professionals/ (accessed Mar 26, 2015).

(5) WHO | Essential leishmaniasis maps http://www.who.int/leishmaniasis/leishmaniasis_maps/en/ (accessed Mar 26, 2015).

(6) CDC - Global Health - Neglected Tropical Diseases http://www.cdc.gov/globalhealth/ntd/ (accessed Mar 26, 2015).

(7) WHO | Innovative and Intensified Disease Management (IDM) http://www.who.int/neglected_diseases/disease_management/en/ (accessed Mar 26, 2015).

(8) Le Pape, P. *J. Enzyme Inhib. Med. Chem.* **2008**, *23*, 708–718.

(9) Newman, D. J.; Cragg, G. M. *J. Nat. Prod.* **2012**, *75*, 311–335.

(10) Pan, L.; Lezama-Davila, C. M.; Isaac-Marquez, A. P.; Calomeni, E. P.; Fuchs, J. R.; Satoskar, A. R.; Kinghorn, A. D. *Phytochemistry* **2012**, *82*, 128–135.

(11) Our, I.; Kinghorn, P. A. D.; Satoskar, A.; Lezama-, C. 129–165.

(12) Hanson, J. R.; Kiran, I.; Scarbrough, C. **2003**, 301–302.

(13) Reich, R.; Keana, J. F. W. *Synth. Commun.* **1972**, *2*, 323–325.

(14) Ainslie_PS MS with Pari_revision-RemovedTracking.

(15) Wang, Z. E.; Reiner, S. L.; Zheng, S.; Dalton, D. K.; Locksley, R. M. *J. Exp. Med.* **1994**, *179*, 1367–1371.

(16) Galvao, J.; Davis, B.; Tilley, M.; Normando, E.; Duchen, M. R.; Cordeiro, M. F. *FASEB J.* **2014**, *28*, 1317–1330.

(17) Rahim, S. S.; Khan, N.; Boddupalli, C. S.; Hasnain, S. E.; Mukhopadhyay, S. *Immunology* **2005**, *114*, 313–321.

(18) Ciechanover, A. *EMBO J.* **1998**, *17*, 7151–7160.

(19) Crawford, L. J.; Walker, B.; Irvine, A. E. *J. Cell Commun. Signal.* **2011**, *5*, 101–110.

(20) Krunic, A.; Vallat, A.; Mo, S.; Lantvit, D. D.; Swanson, S. M.; Orjala, J. *J. Nat. Prod.* **2010**, *73*, 1927–1932.

(21) Hines, J.; Groll, M.; Fahnestock, M.; Crews, C. M. *Chem. Biol.* **2008**, *15*, 501–512.

(22) Kopp, F.; Mahlert, C.; Grünewald, J.; Marahiel, M. a. *J. Am. Chem. Soc.* **2006**, *128*, 16478–16479.